공학석사 학위논문

Structural Approach for High Performance Solution-Processed Organic Solar Cells : Acetylene-incorporated Pyrene Derivatives

파이렌-아세틸렌 구조를 이용한 유기 태양전지의

물질에 관한 연구

2012년 8월

서울대학교 대학원

재료공학부 하이브리드재료전공

문 정 욱

Structural Approach for High Performance Solution-Processed Organic Solar Cells : Acetylene-incorporated Pyrene Derivatives

파이렌-아세틸렌 구조를 이용한 유기 태양전지의
물질에 관한 연구

지도 교수 박 수 영

이 논문을 공학석사 학위논문으로 제출함
2012 년 8 월

서울대학교 대학원
재료공학부 하이브리드재료전공
문 정 욱

문정욱의 석사 학위논문을 인준함
2012 년 8월

위 원 장 _____ (인)

부위원장 _____ (인)

위 원 _____ (인)

Structural Approach for High Performance Solution-Processed Organic Solar Cells : Acetylene-incorporated Pyrene Derivatives

A THESIS FOR MASTER DEGREE
IN ENGINEERING AT THE GRADUATE SCHOOL OF
SEOUL NATIONAL UNIVERSITY

AUGUST 2012

By
Jeong-Wook Mun

Supervisor
Prof. Soo Young Park

학위논문 원문제공 서비스에 대한 동의서

본인의 학위논문에 대하여 서울대학교가 아래와 같이 학위논문 제공하는 것에 동의합니다.

1. 동의사항

① 본인의 논문을 보존이나 인터넷 등을 통한 온라인 서비스 목적으로 복제할 경우 저작물의 내용을 변경하지 않는 범위 내에서의 복제를 허용합니다.
② 본인의 논문을 디지털화하여 인터넷 등 정보통신망을 통한 논문의 일부 또는 전부의 복제.배포 및 전송 시 무료로 제공하는 것에 동의합니다.

2. 개인(저작자)의 의무

본 논문의 저작권을 타인에게 양도하거나 또는 출판을 허락하는 등 동의 내용을 변경하고자 할 때는 소속대학(원)에 공개의 유보 또는 해지를 즉시 통보하겠습니다.

3. 서울대학교의 의무

① 서울대학교는 본 논문을 외부에 제공할 경우 저작권 보호장치(DRM)를 사용하여야 합니다.
② 서울대학교는 본 논문에 대한 공개의 유보나 해지 신청 시 즉시 처리해야 합니다.

학위구분 : 석사 ☑ · 박사 ☐
학 과 : 재료공학부
학 번 : 2010-24053
연 락 처 : 02-880-8330
저 작 자 : 문 정 욱 인)

제 출 일 : 2012 년 8 월 일

서울대학교총장 귀하

Abstract

Structural Approach for High Performance Solution-Processed Organic Solar Cells : Acetylene-incorporated Pyrene Derivatives

Jeong-Wook Mun

Department of Materials Science and Engineering

The Graduate School

Seoul National University

To explore effects of acetylene-incorporation, acetylene-bridged small molecules were successfully synthesized and their photophysical, electrochemical, thermal, and photovoltaic device properties were investigated. The acetylene-incorporation was intended to benefit reduced HOMO-LUMO band gap through extended conjugation, and also the increased ionization potential of the molecules. It is well known that the former is effective in increasing *J*sc, while the latter in increasing *V*oc. Consistent with the expectation and DFT calculation result, acetylene-incorporated pyrene derivatives exhibited planar back-bone, conjugation extension, enhanced light absorption, and low HOMO energy level. Combined with the advanced properties, solution-processed

organic solar cells based on a blend of DPP-A-PY(HD) as a donor and [6,6]-phenyl-C_{71}-butyric-acid-methyl-ester ($PC_{70}BM$) as an acceptor exhibited as high as *V*oc of 0.85V, *J*sc of 8.89 mA cm^{-2}, FF of 41.7% and PCEs of 3.15%.

Keywords : Organic solar cells, Electron donors, Acetylene, Pyrene

Student Number: 2010-24053

Contents

List of Tables

List of Schemes

List of Figures

CHAPTER 1.
Introduction

1-1. Background

In the twentieth century, civilization and economy was rapidly advanced due to mass production and consumption using the fossil fuels. However, the use of fossil fuels resulted in a serious environmental pollution and global warming crisis. So acquiring power from the sun using solar cells as the alternative of fossil fuels has drawn great attention due to their advantages of clean and infinite energy source. Since Becquerel for the first time observed conversion of solar radiation into electricity in 1839[1] and Tang reported organic solar cells (OSCs) device in 1986[2], many researchers have studied the OSCs as alternative way to generate electricity.

At first, organic solar cells contains two different layers as a donor and an acceptor between the conductive electrodes.[3] This two deposited layers forms planar heterojunction and different electrostatic forces are generated at the interface. Local electric field induce dissociation of the excitons and charge transport. However, excitons that do not reach interface recombine and can not contribute to the photocurrent because exciton diffusion length in organic semiconductor is order of 10nm.[4] Recently, to solve this problem, bulk-heterojunction (BHJ) type was designed,

which a donor and an acceptor are mixed.[5] BHJ structure has advantages of a much higher internal interface and similar length scale of blend with exciton diffusion length. Also, OSCs comprised of a bulk-heterojunction (BHJ) layer have drawn great spotlight due to their potential of various advantages such as low cost solar electricity with light-weight devices, and large-area mass production.[6] Solution-processed BHJ OSCs based on bicontinuous networks of polymer donor and fullerene-derivative acceptor have achieved high power conversion efficiencies (PCEs) of more than 6~8%.[7] In parallel with that, OSCs based on small molecule have also received much attention as a promising field due to their advantages such as perfectly defined chemical structure, easy purification, reproducibility without batch to batch variation, and high charge carrier mobility.[8] Although several families of small molecule such as oligothiophene[9], diketopyrrolopyrroles (DPP)[10], and triphenylamine (TPA)[11] show high OSCs device efficiencies, most of the small molecule-based on BHJ OSCs still exhibit low performance.[12]

1-2. Bulk-heterojunction Organic Solar cells (BHJ OSCs)

1-2.1. Operation principles of OSCs

The energy conversion process has six steps in the common mechanism (Figure 1-1).[13] These are; 1. Photon absorption, 2. Exciton formation, 3. Exciton migration, 4. Exciton dissociation, 5. Charge transport, 6. Charge collection at the electrode.

Step 1. Photon absorption

The incoming photons from the sun are absorbed in the active layer. From a materials perspective, it is important to have an absorption coefficient of the active material that matchs the solar irradiation. So during the past decade, there has been continuous researchs for lowering the band gap of materials used.

Step 2. Exciton formation

After optical absorption has occurred, an exiton is formed. The exciton consists of a pair of Coulombically bound electrons and hole pairs.

Step 3. Exciton migration

Then exciton migrate through the material with exciton diffusion length, L_D, typically it is the order of 10nm. Due to the limited L_D, excitons that do not reach interface recombine and can not contribute to the photocurrent.

Step 4. Exciton dissociation

At interface between donor and acceptor, the exciton dissociate into free charge

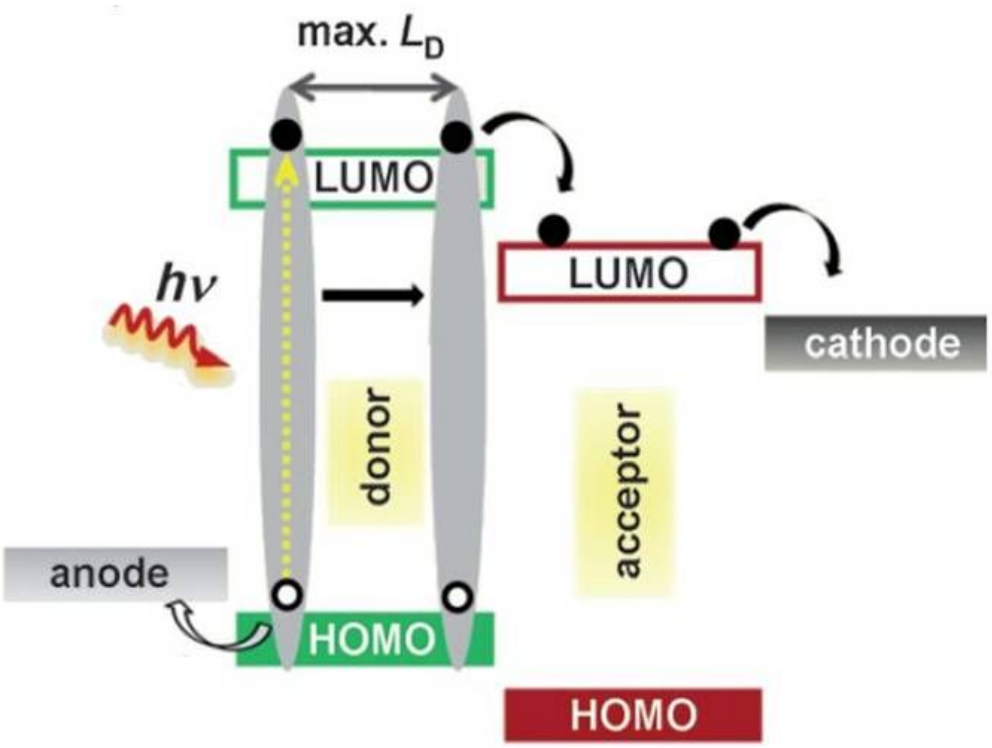

Figure 1-1. Schematic illustration of the physical process of BHJ OSCs.[13]

carriers (an electron and a hole), which is the way of converting the energy emerging from the absorbed photon. The process must be energetically favorable to separate the exciton. Dissociated charge carriers are free to move, or to move and then be trapped (recombination). If the field is too weak for seperation beyond electrostatic attraction, the seperated electrons and holes are merge into an exciton (unimolecular

recombination). Also, an electron and a hole from different excitons are likely to recombine (bimolecular recombination).

Step 5. Charge transport

Electrons and holes have different mobilities in the material, which result in accumulation of one side of charge carriers and thus recombination. So balanced electron- and hole- mobility is important for high current of OSCs.

Step 6. Charge collection at the electrode

If an electron or a hole is present close to an electrode, charge is collected according to barrier penetration mechanisms.

1-2.2. Device characterization[14]

Figure 1-2 shows typical BHJ OSCs configuration. ITO is indium tin oxide and PEDOT:PSS (usally used as hole transporting material, HTL) is poly(3,4-ethylenedioxythiophene)-polystyrene sulfonate. Instead of PEDOT:PSS, MoO_3 (Molybdenum trioxide) is also used for HTL.[15] Organic active layer is located between cathode and anode. The organic layer can be deposited by sublimation under vaccume or coating from a solution. The organic solar cells are based on the charge generation at an interface between organic semiconductors.

The parameters used to characterize the performace of photovoltaic device are *J*sc, *V*oc, FF, η, and IPCE. *J*sc is the short-circuit current; *V*oc is the open-circuit voltage;

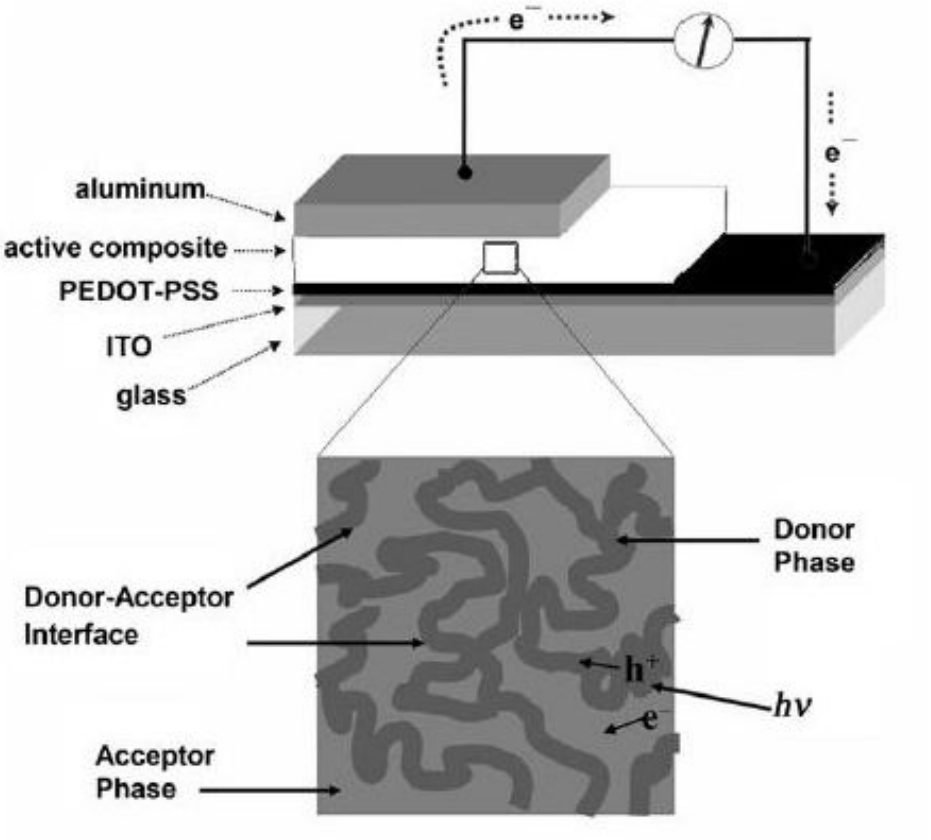

Figure 1-2. Schematic illustration of BHJ OSCs devices.[5-b]

FF is the fill factor; η is the power conversion efficiency; and IPCE is the incident photon conversion efficiency. The fill factor of a device is defined as the ratio between the maximum power delivered to an external circuit and the potential power :

$$FF = Pm / JscVoc = JmVm / JscVoc < 1$$

The fill factor is the ratio of the darkly shaded to lightly shaded regions in Figure 1-3. *V*oc is the sum of the built-in potential (The built-in potential arising from the difference work functions of the cathode and anode) and chemical potential (If the semiconductor absorb the photon, electron and hole are seperated. The seperated charge cause the chemical potential). In the condition of fermi level alignment, current is allowed to travel along the path at non-external electric field. The current flowing the path at this state is *J*sc, which is dependent on the density of charge. the The the incident photon conversion efficiency (IPCE), is given by the number of electrons generated per incident photon:

$$\mathrm{EQE} = n_e / n_{ph} = J_{sc} hc / P_o \lambda e$$

Where P_o is the incident optical power, h is Planck's constant, c is the speed of light, λ is the wavelength of light, and e is the electrical charge.

1-2.3. Bulk-heterojunction concept

The small exciton diffusion length (order of 10nm) of semiconductor limited the photocurrent generation in the region between donors and acceptors. For solving this problem in bilayer type device, the BHJ concepts were introduced to increase the donor-acceptor interface. The interpenetraing donor-acceptor networks can be made by co-evaporation of each molecule or spin coating of binary solution. Figure 1-2 shows the BHJ. The donor phase intimately mixed with the acceptor phase and any phase in

the composite film is within a few nanometers of a neiboring donor-acceptor interface. The quantum efficiency for photoinduced charge separation is same with bilayer type, but the photoelectric conversion efficiency is increased in BHJ concepts.

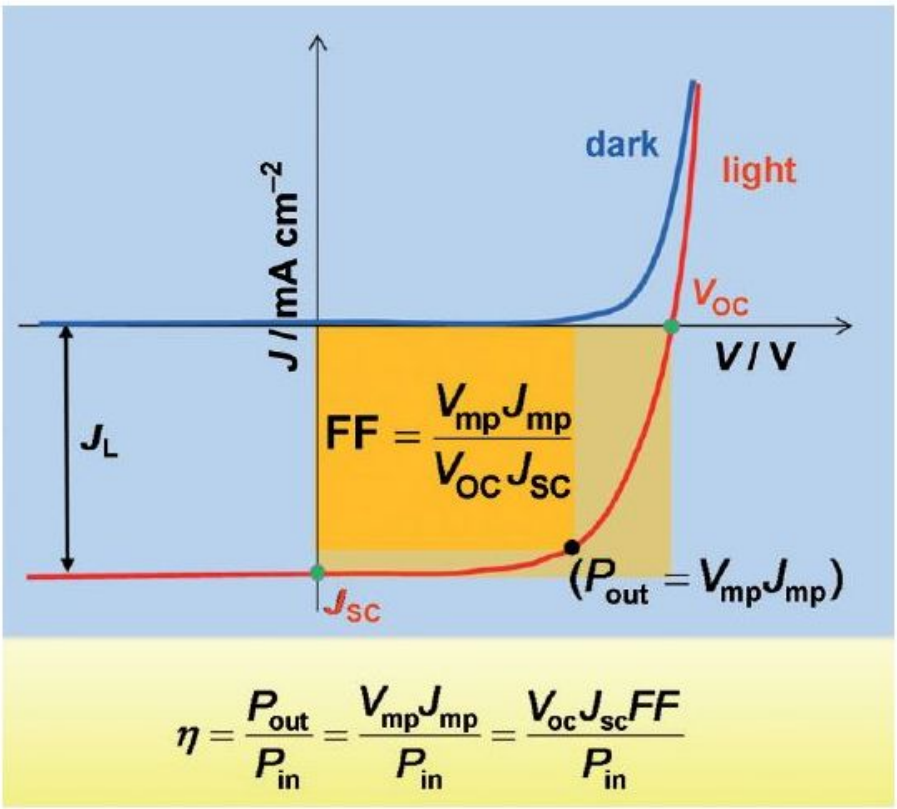

Figure 1-3. Current-voltage (*J*–*V*) characteristics of photovoltaic device under illumination.[13]

1-2.4. Recent research trends in solution processible small molecule donors

With the considerable efforts to develop high performace solution processible small molecule donors, many materials have been synthesized and characterized in OSCs. Because the side or end alky chain affect to not only solubility but also packing structure with fullerenes, many researchers consider the factors in designing the materials.[16] In point of view of a group of materials, such as oligothiophene[9], DPP[10], TPA[11], other donor (D) – acceptor (A) type molecules[12], and dye molecules[12] have been reported.

Yongsheng Chen, *et al*. reported interesting result about thiophene-based small molecules end-capped with alkyl cyanoacetate groups (Figure 1-4).[17] They designed 3 structures having various length of alkyl chain (ethyl, octyl, and ethylhexyl). They showed the good solubility and film forming property than previous reported dicyanovinyl group containing molecule.[8-b] This materials exhibited interpenetraing networks with $PC_{60}BM$, thus charge carrier collection efficieny was increased. A PCEs of 5.08% was achieved based on structure with octyl side chain and $PC_{60}BM$. (J_{sc}=10.74 mA cm^{-2}, V_{oc}=0.86V, FF=55.0%)

Thuc-Quyen Nguyen, *et al*. reported small molecules based on DPP group.[10] The DPP core shows the self-assembled to odered domain and low band gap with other component. They exhibit various properties according to alkyl chains on the *N*,*N*-

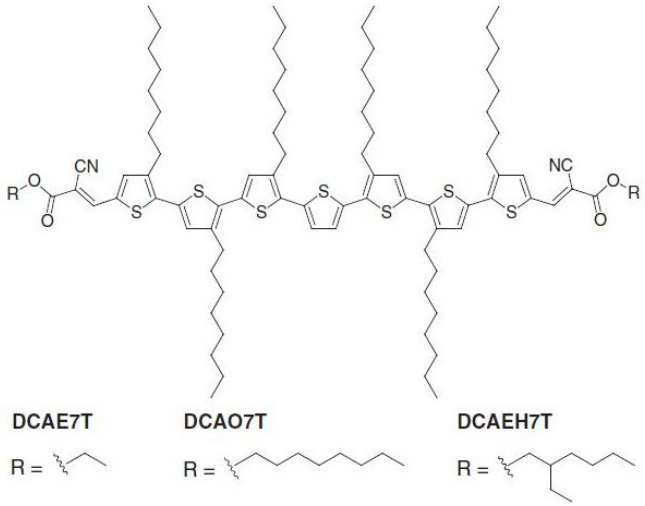

Figure 1-4. Schemes of thiophene-based small molecules end-capped with alkyl cyanoacetate groups.[17]

positions of the lactam rings. DPP-oligothiophene (Figure 1-5a) with $PC_{70}BM$ shows PCEs=3.0% (J_{sc}=9.2 mA cm^{-2}, V_{oc}=0.75V, FF=44%). The optical, electronic and molecular packing properties could be controlled by changing the substituents. (Figure 1-5b)

Alan J. Heeger *et, al*. reported a new small molecule donor with PCEs of 6.7% under AM 1.5G irradiation (100 mW cm^{-2}) (Figure 1-6). This A-D-A type molecule promote intramolecular π-delocalization and intramolecular π-π stacking, and thereby shows the high charge carrier mobility (0.12 cm^2 V^{-1} S^{-1}, On/off ratio of ~10^7). In device

fabrication, small amount of solvent additive (1,8-diiodooctane) result in improvement of performance due to small domain size (from 20~30nm to 15~20nm).

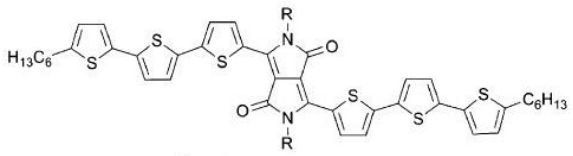

a) R : Ethylhexyl

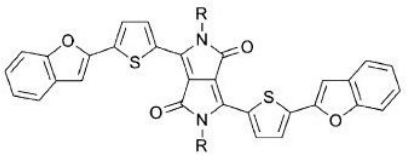

b) R : Ethylhexyl

Figure 1-5. Schemes of DPP-based small molecules.[10] The b) structure exhibits PCEs=4.2% (J_{sc}=9.0 mA cm^{-2}, V_{oc}=0.94V, FF=49%).

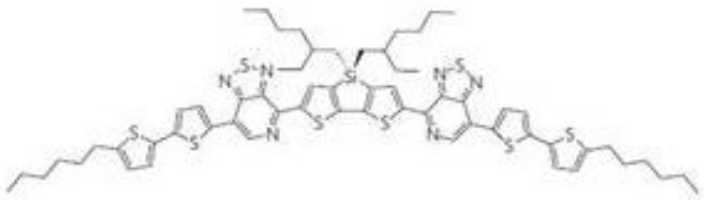

Figure 1-6. Schemes of A-D-A type small molecules.[18]

1-3. References

1. Becquerel, A. E. *C. R. Hebd. Seances Acad. Sci.* **1839**, 561.

2. Tang, C. W. *Appl. Phys. Lett.* **1986**, 48, 183.

3. (a) Sariciftci, N. S.; Braun, D.; Zhang, C.; Srdanov, V. I.; Heeger, A. J.; Stucky, G.; Wudl, F. *Appl. Phys. Lett.* **1993**, 62, 585. (b) Halls, J. J. M.; Pichler, K.; Friend, R. H.; Moratti, S. C.; Holmes, A. B. *Appl. Phys. Lett.* **1996**, 68, 3120. (c) Alam, M. M.; Jenekhe, S. A. *Chem. Mater.* **2004**. 16. 4647.

4. (a) Scully, S. R.; McGehee, M. D. *J. Appl. Phys.* **2006**, 100, 034907. (b) Brabec, C. J.; Sariciftci, N. S.; Hummelen, J. C. *Adv. Funct. Mater.* **2001**, 11, 15.

5. (a) Yu, G.; Gao, J.; Hummelen, J. C.; Wudl, F.; Heeger, A. J. *Science.* **1995**, 270, 1789. (b) Thompson, B. C.; Frechet, J. M. *Angew. Chem. Int. Ed.* **2008**, 47, 58. (c) Cheng, Y. J.; Yang, S. H.; Hsu, C. S. *Chem. Rev*. **2009**, 109, 5868. (d) Huo, L. J.; Hou, J. H.; Zhang, S. Q.; Chen, H. Y.; Yang, Y. *Angew. Chem. Int. Ed*. **2010**, 49, 1500.

6. (a) Gunes, S.; Neugebauer, H.; Sariciftci, N. S. *Chem. Rev*. **2007**, 107, 1324. (b) Park, S. H.; Roy, A.; Beaupre, S.; Cho, S.; Coates, N.; Moon, J. S.; Moses, D.; Leclerc, M.; Lee, K.; Heeger, A. J. *Nat. Photon.* **2009**, 3, 297. (c) Liang, Y.; Xu, Z.; Xia, J. B.; Tsai, S. T.; Wu, Y.; Li, G.; Ray, C.; Yu, L. P.; *Adv. Mater.* **2010**, 22, E135. (d) Liang, Y.; Yu, L.; *Acc. Chem. Re.* **2010**, 43, 1227.

7. (a) Zhou, H.; Yang, L.; Stuart, A. C.; Price, S. C.; Liu, S.; You, W. *Angew. Chem. Int. Ed*. **2011**, 50, 2995. (b) Chu, T.-Y.; Lu, J.; Beaupre, S.; Zhang, Y.; Pouliot, J. -R.; Wakim, S.; Zhou, J.; Leclerc, M.; Li, Z.; Ding, J.; Tao, Y. *J. Am. Chem. Soc.* **2011**, 133, 4250. (c) Price, S. C.; Stuart, A.; Yang, L.; Zhou, H.; You, W. *J. Am. Chem. Soc.* **2011**, 133, 4625. (d) Boudreault, P. -L. T.; Najari, A.; Leclerc, M. *Chem. Mater.* **2011**, 23, 456.

8. (a) Roncali, J. *Acc. Chem. Res.* **2009**, 42, 1719. (b) Walker, B.; Kim, C.; Nguyen, T. -Q. *Chem. Mater.* **2011**, 23, 470.

9. Liu, Y.; Wan, X.; Yin, B.; Zhou, J.; Long, G.; Yin, S.; Chen, Y. *J. Mater. Chem.* **2010**, 20, 2464.

10. (a) Tamayo, A. B.; Walker B.; Nguyen, T. Q. *J. Phys. Chem. C.* **2008**, 112, 11545. (b) Walker, B.; Tamayo, A. B.; Dang, X. D.; Zalar, P.; Seo, J. H.; Garcia, A.; Tantiwiwat, M.; Nguyen, T. Q. *Adv. Funct. Mater.* **2009**, 19, 3063.

11. (a) Shang, H.; Fan, H.; Liu, Y.; Hu, W.; Li, Y.; Zhan, X. *Adv. Mater.* **2011**, 23, 1554. (b) Zhang, J.; Deng, D.; He, C.; He, Y. J.; Zhang, M. J.; Zhang, Z. G.; Zhang, Z. J.; Li, Y. F. *Chem. Mater.* **2011**, 23, 817.

12. (a) Winzenberg, K. N.; Kemppinene, P.; Fanchini, G.; Bown, M.; Collis, G. E.; Forsyth, C. M.; Hegedus, K.; Singh, T. B.; Watkins, S. E. *Chem. Mater.* **2009**, 21, 5701. (b) Bagnis, D.; Beverina, L.; Huang, H.; Silvestri, F.; Yao, Y.; Yan, H.; Pagani, G. A.; Marks, T. J.; Facchetti, A. *J. Am. Chem. Soc.* **2010**, 132, 4074. (c) Burckstummer, H.; x Kronenberg, H.; Gsanger, M.; Stolte, M.; Meerholz, K.; Wurthner, F. *J. Mater. Chem.*

2010, 20, 240. (d) Rousseau, T.; Cravino, A.; Ripaud, E.; Leriche, P.; Rihn, S.; De Nicola, A.; Ziessel, R.; Roncali, J. *Chem. Commun.* **2010**, 46, 5082.

13. Mishra, A. Bauerle, P. *Angew. Chem. Int. Ed*. **2012**, *51*, 2020.

14. Sun, S. –S.; Sariciftci, N. S. *Organic photovoltaics ; Mechanism, Materials, and Devices.*

15. Lin, H. –W.; Lin, L. –Y.; Chen, Y. –H.; Chen, C. –W.; Lin, Y. –T.; Chiu, S. –W.; Wong, K. –T. *Chem. Commun.* **2011**, 47, 7872.

16. (a) Thompson, B. C.; Kim, B. J.; Kavulak, D. F.; Sivula, K.; Mauldin, C.; Frechet, J. M. J. *Macromolecules*. **2007**, 40, 7425. (b) Johns, J. E.; Muller, E. A.; Frechet, J. M. J.; Harris, C. B. *J. Am. Chem. Soc.* **2010**, 132, 15720.

17. Liu, Y. S.; Wan, X. J.; Wang, F.; Zhou, J. Y.; Long, G. K.; Tian, J. G.; You, J. B.; Yang, Y.; Chen, Y. S. *Adv. Energy Mater.* **2011**, 1, 771.

18. Sun, Y. M.; Welch, G. C.; Leong, W. L.; Takacs, C. J.; Bazan, G. C.; Heeger, A. J. *Nature Materials.* **2012**, 11, 44.

CHAPTER 2.
Tetra-functionalized Pyrene Derivatives for Bulk-heterojunction Organic Solar Cells

2-1. Introduction

For the higher photovoltaic efficiencies in small molecule OSCs, high charge transport property is essential because of the low interpenetration through the active layer.[1] Conjugated acene molecules have been exhibited high charge-carrier mobility [2], which may be attributed to intermolecular arrangement and large exciton diffusion length, desirable for balanced hole and electron transport in BHJ OSCs. Such as hexa-peri-hexabenzocoronene (HBC) and its derivatives have been shown high charge-carrier mobility because of the self-assembled columnar structure and exhibited potential applications as an active component for OSCs.[3] Acetylene group reduces the steric hindrance and makes planar molecular structure.[4] This planarity of small molecule induces π-π intermolecular interaction, therefore acetylene-incorporated compound shows enhanced charge-carrier mobility and photovoltaic performance.

Pyrene has been widely studied due to their excellent fluorescent properties, which enabled the application in fluorecent probes or fluorescent sensor.[5] Recently, some pyrene derivatives have been developed as electronic materials in the field of organic

light emitting diode[6], organic field-effect transistors (OTFTs)[7], and OSCs[8]. From the point of view of structure, pyrene has a rigid and planar aromatic ring and thereby shows good tendency to self-assembled into ordered domain. As a result, pyrene-based materials would exhibited high charge carrier mobility and thus potential for application in OTFTs and OSCs. Herein, we report the design, synthesis and charaterization of acetylene-incorporated pyrene derivative, which was designed with several concepts. 1) The electrophilic substitution of pyrene takes place mainly at the 1,3,6, and 8-position based on experimental and calculation results.[9] The electrophile attacks the aromatic ring, forming positively charged intermediate state (rate-determining step), and finally leaving group is detached in arenium ion mechanism. This position exhibited low intermediate state energy in rate-determining step, thus 1,3,6, and 8-tetrafunctionalized pyrenes have the advantage of easy synthesis for various application. 2) We report the new D-A type small molecule with 1,3,6, and 8-tetrafunctionalized pyrene as donor (D) unit and dicyanovinyl or octyl cyanoacetate group as acceptor (A) unit for the first time. The dicyanovinyl and octyl cyanoacetate group has strong withdrawing character and thereby can lead to efficient intramolecular charge transfer for reducing the optical band-gap, desirable for light absorption at longer wavelength. 3) Acetylene π-spacer between thienylene and pyrene group would result in more planar structure, which would facilitates the internal charge transfer between electron-donating and electron-withdrawing group, and

intermolecular arrangement. So acetylene-incorporated pyrene derivatives would show enhanced charge-carrier mobility and solar cells performance.

2-2. Experimental

2-2.1. Synthesis

The molecular structures of target materials are shown in Scheme 2-1. All reagents were purchased from Sigma Aldrich, TCI, and Alfa Aesar. The final products, PY1 and PY2, were produced through Pd-catalyzed Suzuki and Sonogashira coupling reactions, respectively. Compound 1 was obtained through sonogashira reaction with 1,3,6,8-tetrabromopyrene and trimethylsilylacetylene. Then product was treated with K_2CO_3 in MeOH and $CHCl_3$ to afford compound 2. Compound 3 was synthesiszed through bromination with NBS. Compound 5 was also obtained through sonogashira reaction with 1,3,6,8-tetraethynylpyrene (4) and 5-bromo-3-hexylthiophene-2-carbaldehyde (2). The final product, PY3 and PY3-1, were prepared by knoevenagel reaction of compound (5) with malononitrile and octyl cyanoacetate, respectively.

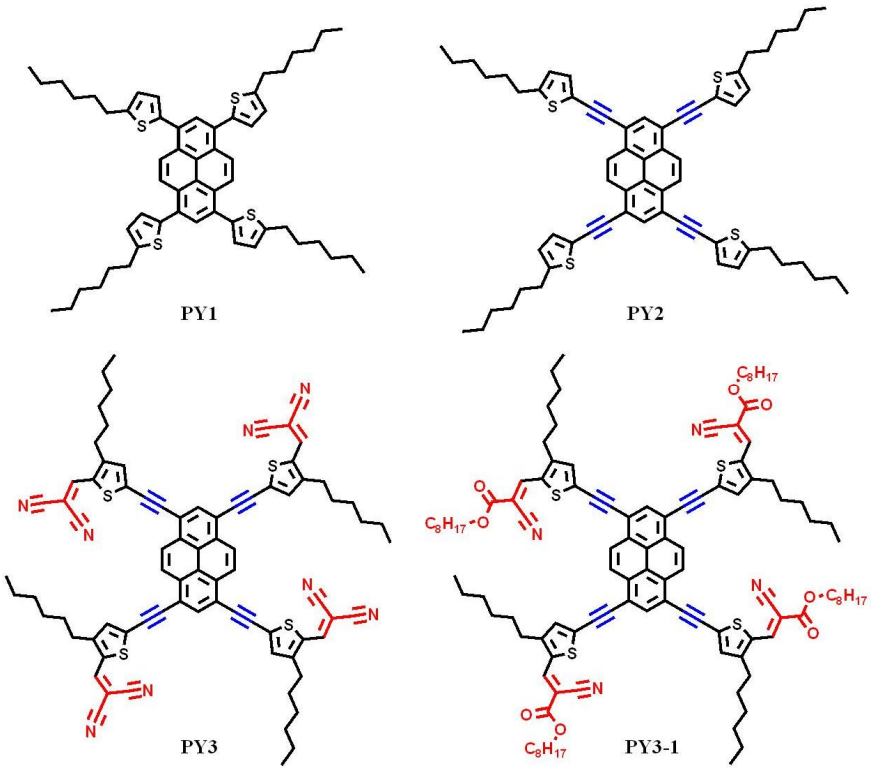

Scheme 2-1. Chemical structures of PY1~PY3-1.

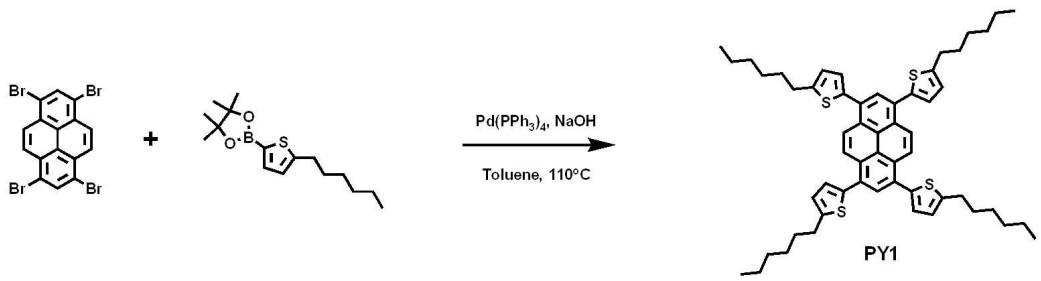

Scheme 2-2. Synthesis of PY1.

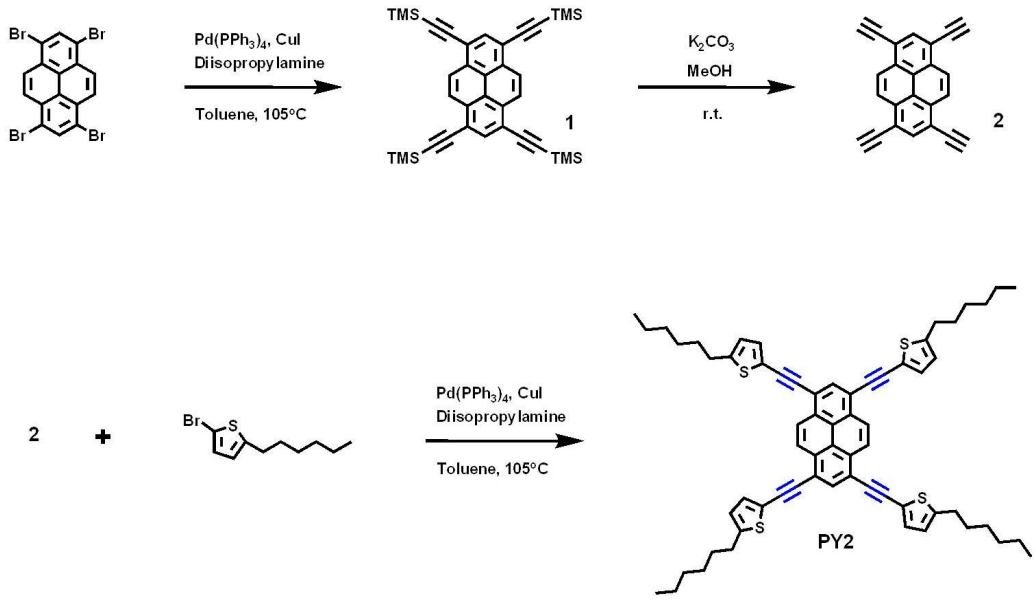

Scheme 2-3. Synthesis of PY2.

1,3,6,8-tetrakis(5-hexylthiophen-2-yl)pyrene (PY1)

1,3,6,8-Tetrabromopyrene (170mg, 0.33mmol), 2-(5-hexylthiophen-2-yl)-4,4,5,5-tetramethyl-1,3,2-dioxaborolane (500mg, 1.3286mmol), $Pd(PPh_3)_4$ (77mg, 0.04mmol), toluene (35ml), EtOH (12ml), and NaOH(2N) (15ml) were added to a two-necked round bottom flask under Ar atmosphere. The solution was stirred at 110℃ for 24h. The mixture was poured into water and extracted with $CHCl_3$. The organic layer was then dried over anhydrous $MgSO_4$. After evaporation of the solvent,

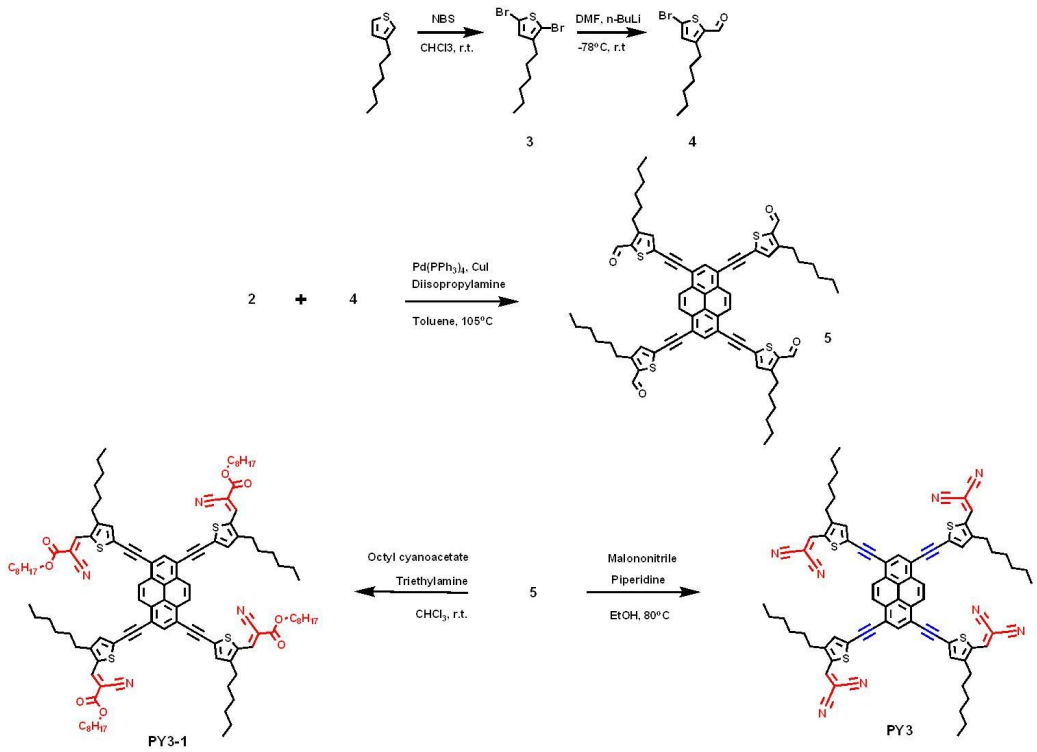

Scheme 2-4. Synthesis of PY3 and PY3-1

the residue was purified by column chromatography on a silica gel ($CHCl_3$/n-Hex = 1:4) to afford a orange red solid (290mg, 73%). ^{1}H NMR (300MHz, $CDCl_3$, δ) : 8.54 (s, 4H), 8.18 (s, 2H), 7.19 (d, 4H), 6.90 (d, 4H), 2.91 (t, 8H), 1.82-1.73 (m, 8H), 1.48-1.34 (m, 24H), 0.91 (m, 12H). ^{13}C NMR (500MHz, $CDCl_3$, δ) : 147.2, 139.4, 130.8, 130.0, 128.7, 127.9, 126.1, 125.5, 124.4, 31.7, 30.3, 28.9, 22.6, 14.0. High-resolution mass spectrometry (HRMS) (electron ionization (EI)) mass-to-charge ratio (m/z) : M+

calculated for $C_{56}H_{66}S_4$, 866.40 ; found 866.40. Elemental Analysis calculated for $C_{56}H_{66}S_4$: C 77.54, H 7.67, S 14.79 ; found: C 77.45, H 7.79, S 14.79.

1,3,6,8-tetrakis((trimethylsilyl)ethynyl)pyrene (1)

The mixture of 1,3,6,8-Tetrabromopyrene (1.0g, 1.93mmol), $Pd(PPh_3)_4$ (0.136g, 0.19mmol), and CuI (36.8mg, 0.19mmol) in DIPA(12ml) and Toluene(20ml) were stirred under Ar atmosphere for 10min. Then TMSA (1.62ml, 11.58mmol) was added to the mixture and stirred at 80℃ for 24h. After evaporation of the solvent, the residue was purified by column chromatography on a silica gel (n-Hex) to afford a red orange solid (650mg, 57%). ^{1}H NMR (300MHz, $CDCl_3$, δ) : 8.53 (s, 4 H), 8.28 (s, 2 H), 0.39 (s, 36 H).

1,3,6,8-tetraethynylpyrene (2)

To a solution of 1,3,6,8-tetrakis((trimethylsilyl)ethynyl)pyrene (1) (500mg, 0.85mmol) in MeOH (20ml) and $CHCl_3$ (60ml) was treated with K_2CO_3 (0.64g, 4.69mmol). The solution was stirred for 8h at room temperature. After removing the solvent, the residue was purified by column chromatography on a silica gel ($CHCl_3$) and recrystallized to afford a light-yellow solid (0.83g, 92%). ^{1}H NMR (300MHz, $CDCl_3$, δ) : 7.09 (d, 1H), 6.63 (d, 1H), 3.28 (s, 1H), 2.79-2.74 (t, 2H), 1.67-1.25 (m, 8H), 0.90-0.86 (m, 3H).

1,3,6,8-Tetrakis((5-hexylthiophen-2-yl)ethynyl)pyrene (PY2)

2-bromo-5-hexylthiophene (1.8g, 7.38mmol), CuI (95mg, 0.50mmol), and $Pd(PPh_3)_4$ (580mg, 0.50mmol) in DIPA(30ml) and Toluene(60ml) were stirred under Ar atmosphere at 0℃ for 30min. 1,3,6,8-tetraethynylpyrene (2) was then added, and the mixture was heated to 60 °C for 36 h. The mixture was poured into water and extracted with $CHCl_3$. The organic layer was then dried over anhydrous $MgSO_4$. After evaporation of the solvent, the residue was purified by column chromatography on a silica gel (CHCl3/n-Hex = 1:9) to afford a red solid (1.1g, 20%). ^{1}H NMR (300MHz, $CDCl_3$, δ) : 8.66 (s, 4H), 8.35 (s, 2H), 7.28 (d, 4H), 6.77 (d, 4H), 2.86 (t, 8H), 1.78-1.68 (m, 8H), 1.41-1.33 (m, 24H), 0.91 (m, 12H). ^{13}C NMR (500MHz, $CDCl_3$, δ) : 149.4, 133.1, 132.7, 131.6, 126.9, 124.7, 124.3, 120.6, 119.0, 91.0, 90.1, 31.7, 30.5, 28.9, 22.8, 14.3. High-resolution mass spectrometry (HRMS) (electron ionization (EI)) mass-to-charge ratio (m/z) : M+ calculated for $C_{64}H_{66}S_4$, 963.41 ; found 963.41. Elemental Analysis calculated for $C_{64}H_{66}S_4$: C 79.72, H 6.90, S 13.31 ; found: C 79.72, H 6.84, S 13.37.

2,5-dibromo-3-hexylthiophene (3)

NBS (8.5g, 47.5mmol) was added dropwisely to the solution of 3-hexylthiophene (1g, 5.94mmol) in $CHCl_3$ (200ml) under exclusion of light. The mixture was slowly heated to room temperature and stirred for 48h. The solution was poured into water and

extracted with MC. The organic layer was then dried over anhydrous $MgSO_4$. After removing the solvent, the residue was purified by column chromatography on a silica gel (n-Hex) to afford a light-yellow oil (1.7g, 87%). ^1H NMR (300MHz, $CDCl_3$, δ) : 6.77 (s, 1H), 2.50 (t, 2H), 1.52 (m, 2H), 1.36-1.25 (m, 9H).

5-bromo-3-hexylthiophene-2-carbaldehyde (4)

2,5-dibromo-3-hexylthiophene (1) (2.5g, 7.66 mmol) was mixed with dry THF (200 mL). This mixture was added with n-butyllithium (4.8 mL, 1.6 M in hexane, 7.66 mmol) dropwise at -78℃ under argon. After the addition was finished, the mixture was stirred for another 1 h and anhydrous *N*,*N*-DMF (0.65ml, 8.43 mmol) was added into solution. The mixture was slowly warmed to room temperature overnight and poured into 1 N HCl. The organic layer was extracted with $CHCl_3$ and dried over $MgSO_4$. The product was purified by column chromatography on silica gel (EA/n-Hex = 1:9) to afford light brown oil (1.5g, 71%). ^1H NMR (300MHz, $CDCl_3$, δ) : 9.75 (s, 1H), 7.45 (s, 1H), 2.59 (t, 2H), 1.69-1.54 (m, 3H), 1.32 (m, 5H), 0.91-0.87 (m, 3H).

5,5',5'',5'''-(pyrene-1,3,6,8-tetrayltetrakis(ethyne-2,1-diyl))tetrakis(3-hexylthiophene-2-carbaldehyde) (5)

5-bromo-3-hexylthiophene-2-carbaldehyde (4) (812mg, 2.94mmol), CuI (38mg, 0.20mmol), and $Pd(PPh_3)_4$ (232mg, 0.20mmol) in DIPA(10ml) and toluene(22ml) were

stirred under Ar atmosphere at 0℃ for 30min. 1,3,6,8-tetraethynylpyrene (2) was then added, and the mixture was heated to 60 °C for 36 h. The mixture was poured into 1 N HCl and extracted with $CHCl_3$. The organic layer was then dried over anhydrous $MgSO_4$. After evaporation of the solvent, the residue was purified by column chromatography on a silica gel ($CHCl_3$) to afford a violet solid (450mg, 62%). ^1H NMR (300MHz, $CDCl_3$, δ) : 9.90 (s, 4H), 8.68 (s, 4H), 8.42 (s, 2H), 7.65 (s, 4H), 2.99-2.94 (t, 8H), 1.87-1.77 (m, 8H), 1.52-1.27 (m, 24H), 0.89-0.84 (t, 12H).

2,2',2'',2'''-(5,5',5'',5'''-(pyrene-1,3,6,8-tetrayltetrakis(ethyne-2,1-diyl))tetrakis(3-hexylthiophene-5,2-diyl))tetrakis(methan-1-yl-1-ylidene)tetramalononitrile (PY3)

To as solution of 5,5',5'',5'''-(pyrene-1,3,6,8-tetrayltetrakis(ethyne-2,1-diyl))tetrakis(3-hexylthiophene-2-carbaldehyde) (5) (0.2g, 0.18mmol) and molononitrile (59mg, 0.89mmol) in EtOH (50ml) was added piperidine (1drop). The solution was heated at 85°C for 1 h. The mixture was poured into water and extracted with chloroform. The organic layer was then dried over anhydrous $MgSO_4$. After evaporation of the solvent, the residue was purified by column chromatography on a silica gel (EA/$CHCl_3$ = 2:1) and recrystallized to afford a black solid (20mg, 10%). ^1H NMR (300MHz, $CDCl_3$, δ) : 8.74 (s, 4H), 8.47 (s, 2H), 7.79 (s, 4H), 7.64 (s, 4H), 2.98 (t, 8H), 1.85-1.82 (m, 8H), 1.49-1.39 (m, 24H), 0.89-0.87 (t, 12H). Elemental Analysis calculated for $C_{80}H_{66}N_8S_4$: C 75.80, H 5.25, N 8.84, S 10.12; found: C 75.32, H 5.25, N 8.85, S 10.04.

(2E,2'E,2''E,2'''E)-tetraoctyl 3,3',3'',3'''-(5,5',5'',5'''-(pyrene-1,3,6,8-tetrayltetrakis(ethyne-2,1-diyl))tetrakis(3-hexylthiophene-5,2-diyl))tetrakis(2-cyanoacrylate) (PY3-1)

To as solution of 5,5',5'',5'''-(pyrene-1,3,6,8-tetrayltetrakis(ethyne-2,1-diyl))tetrakis(3-hexylthiophene-2-carbaldehyde) (5) (0.310g, 0.28mmol) and in $CHCl_3$ (500ml) was added piperidine (3drop) and octyl cyanoacetate (2.16g, 10.95mmol). The solution was stirred at r.t. for 80h. The mixture was poured into water and extracted with chloroform. The organic layer was then dried over anhydrous $MgSO_4$. After evaporation of the solvent, the residue was purified by column chromatography on a silica gel ($CHCl_3$) and recrystallized to afford a black solid (300mg, 59%). ^{1}H NMR (300MHz, $CDCl_3$, δ) : 8.66 (s, 4H), 8.38 (s, 2H), 8.23 (s, 4H), 7.66 (s, 4H), 4.34 (t, 8H), 2.97 (t, 8H), 1.83-1.72 (m, 16H), 1.48-1.30 (m, 72H), 0.89-0.83 (t, 16H). ^{13}C NMR (500MHz, $CDCl_3$, δ) : 162.6, 149.5, 145.3, 137.8, 135.9, 133.6, 131.5, 127.3, 123.4, 118.4, 115.7, 99.3, 89.1, 66.7, 31.7, 30.4, 29.7, 29.1, 28.5, 25.8, 22.6, 14.1. Elemental Analysis calculated for $C_{112}H_{134}N_4O_8S_4$: C 75.04, H 7.53, N 3.13, O 7.14, S 7.16; found: C 75.09, H 7.55, N 3.08, O 7.10, S 7.13.

2-2.2. Instruments and measurements

Chemical structures were fully identified by ^{1}H NMR (Bruker, Avance-300), ^{13}C NMR (Bruker, Avance 500), GC-Mass (JEOL, JMS-700), and elemental analysis (EA1110, CE Instrument). The melting temperatures of the compounds were determined using DSC under an N_2 atmosphere, using a TA instruments Q1000 model. The decomposition temperatures of the compounds were obtained using TGA under an N_2 atmosphere, using a TA instruments Q50 model. UV-Vis spectra were recorded on a SHIMADZU UV-1650PC. HOMO level was obtained from the cyclic voltammetry measurements. Cyclic voltammetric measurements were performed using a 273A (Princeton Applied Research) with a one-compartment electrolysis cell consisting of a platinum working electrode, a platinum wire counter-electrode, and a quasi Ag+/Ag electrode as reference. Measurements were performed in a 0.5 mM acetonitrile solution with tetrabutylammonium tetrafluoroborate as the supporting electrolyte, at a scan rate of 50 mV/s. Each oxidation potential was calibrated using ferrocene as a reference. LUMO level was calculated from the HOMO level and the optical band gap, which was obtained from the edge of the absorption spectra.

2-2.3. Fabrication and characterization of organic solar cells (OSCs)

The organic solar cells in this study were fabricated by following method. Patterned ITO glass substrates (~10Ω/square) were cleaned in an ultrasonic bath with trichloroethylene, acetone, isopropyl alcohol, for 10 minute, respectively and then blow dried with a N_2 stream. A 30nm of PEDOT:PSS (AI P 4083) was then spin-coated on to the substrate (5000rpm / 30s). The films were dried at 150°C for 20min. Subsequently, the PY series : $PC_{70}BM$ (> 99.0%, ADS)) solutions were deposited through spin casting at 1000 rpm / 40s. The thickness of PY series : $PC_{70}BM$ films were around 100 nm. Al electrodes were deposited via thermal evaporation with thickness of 100nm. The active area of these solar cells was 0.09 cm^2.

The current density-voltage (*J-V*) characteristics of the solar cells were measured with a Keithley 4200 source measurement unit. The solar cell performances were characterized under AM1.5G condition with an illumination intensity of 100 mW cm^{-2} generated by a Oriel Sol 3A solar simulator. *J-V* characteristics of the cells with illumination were measured using a metal mask of 0.09 cm^2. The intensity dependent measurements have been performed with various neutral density filters.

Incident photon to current conversion efficiency (IPCE) was measured using Oriel QE/IPCE Measurement Kit which composed of 300W Xenon Lamp, monochromator (74125), the order sorting filter wheel, the Merlin lock-in amplifier (70104) and the chopper.

2-3. Result and Discussion

2-3.1. Density functional theory (DFT) calculation

Theoretical molecular orbital calculation was carried out using Gaussian03 at B3LYP/6-31G* level to characterize optimized ground state geometry and electron density of HOMO and LUMO states. In ground optimized geometry (Figure 2-1), PY1 has non-coplanar twisted conformation due to large torsion angle about 41~46° between pyrene core and thiophene moiety which is more distorted than abount 0.1~0.2° between pyrene core and acetylene moiety in PY2. This structural planarity helps π-π intermolecular interaction and crystal formation between neighboring molecules, and thus would enhanced charge-carrier mobility in PY2 compared to PY1. The coplanarity would also facilitates the internal charge transfer between electron-donating pyrene group and electron-withdrawing dicyanovinyl / octyl cyano acetate group in PY3 and PY3-1.

(a) Top view

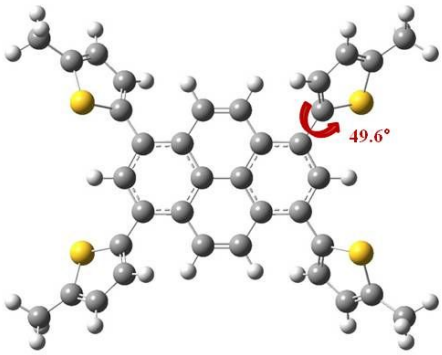

PY1

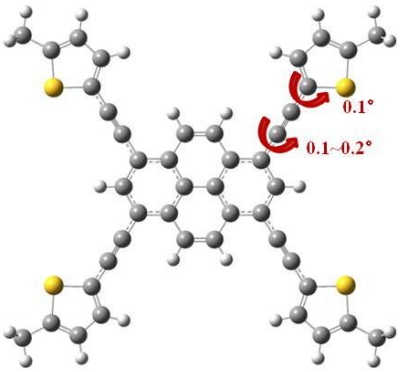

PY2

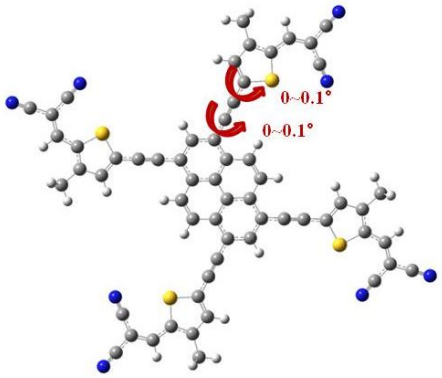

PY3

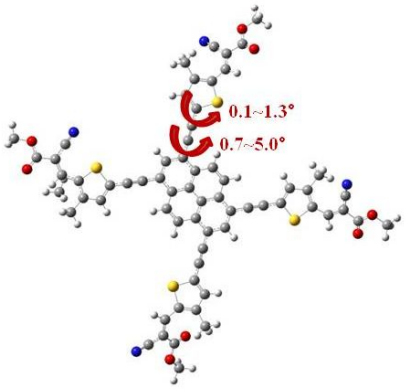

PY3-1

(b) Front view

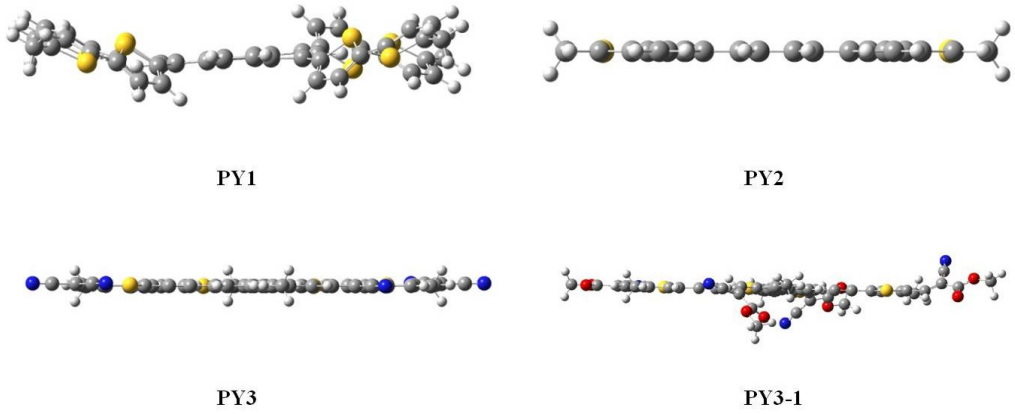

Figure 2-1 The calculated optimized ground state geometry of PY1~PY3-1. (a) Top view and (b) front view obtained using Gaussian 09 at the B3LYP/6-31G* level.

2-3.2. Optical properties

Figure 2-2 shows the normalized UV-Vis absorption spectra of PY1~PY3-1 in $CHCl_3$ solution and spincoated film from $CHCl_3$ solution; Table 2-1 lists the measured data. The film spectra of compounds show red-shifted wavelength absorption relative to solution spectra, which can be structural reorganization in solid state. The film absorption of PY1 and PY2 extends up to 465nm and 555nm in comparison with unsubstituted pyrene due to their extended conjugation system. Distinctive absorption at 500nm in PY2 indicate that acetylene π-spacer result in more planar structure and thereby induced enhanced the π-π intermolecular interactions. The film absorption of PY3 and PY3-1 shows broad absorption extended to ~700nm. When mixed with the fullerene acceptor, the resulting blended film would give a overall spectral overlap in visible region. Broad absorption in PY3 and PY3-1 also indicate that acetylene π-spacer result in more planar structure and thereby induced strong intermolecular interactions. The optical band gap estimated from the absorption edge of PY2 (2.23 eV) in thin film is narrower than that of PY1 (2.66 eV). Bathochromically shifted absorption onset and narrowed optical band gap of PY2 in film state is due to relatively extended conjugation length. Thus acetylene-incorporated PY3 and PY3-1 would enhance internal charge transfer between pyrene and dicyanovinyl or octyl cyano acetate unit.

(a) In solution

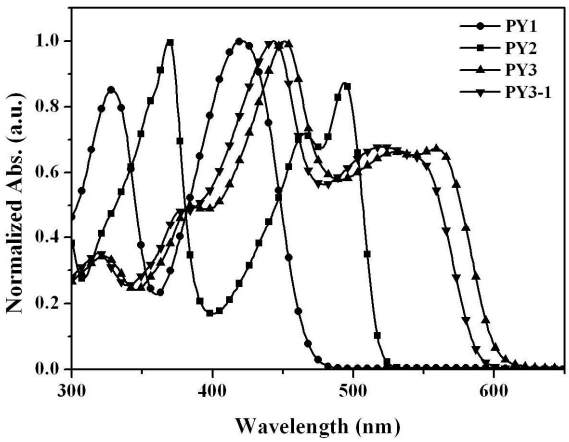

(b) In film

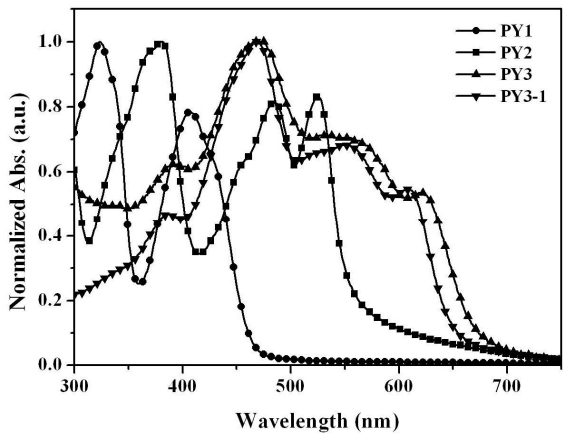

Figure 2-2. The normalized UV-Vis absorption spectra of compound PY1~PY3-1 in (a) $CHCl_3$ solution and (b) spincoated film from $CHCl_3$ solution.

Table 2-1. Optical properties of PY1~PY3-1.

Compound	$\lambda_{abs,sol}$ [a] (nm)	$\lambda_{abs,film}$ [b] (nm)	$\lambda_{onset,film}$ (nm)	$\lambda_{g,film}$ [c] (eV)
PY1	329, 422	324, 408	465	2.66
PY2	369, 466, 504	381, 485, 525	555	2.23
PY3	385, 451, 558	391, 471, 621	672	1.84
PY3-1	319, 378, 443, 520	388, 470, 552, 610	648	1.91

a) Measured in chloroform solution of concentration of 10^{-5}M. b) Spin-coated from 0.5wt% chloroform solution. c) Optical band gap was obtained from film absorption edge.

2-3.3. Electrochemical properties

Measurements were performed using film (dropcasted on ITO) in a 0.5 mM acetonitrile solution with tetrabutylammonium tetrafluoroborate as the supporting electrolyte, at a scan rate of 50 mV/s. HOMO energy level was calculated by comparison with ferrocene (4.8eV), E_{HOMO} = [- (E_{Onset} - $E_{Ferrocene}$) - 4.8], (Figure 2-3) and LUMO energy level was calculated from optical band gap and HOMO energy level. The data are summarized in Table2-2. The HOMO/LUMO energy levels of

PY1~PY3-1 were -5.57/-5.60/-5.41/-5.73 eV and -2.91/-3.37/-3.57/-3.82 eV, respectively, which are appropriate for donor materials. The introduction of acetylene moiety between pyrene and thienylene group lowers the HOMO energy level beneficial for high *V*oc and decreased the band gap by extended conjugation.

Table 2-2. Electrochemical properties of PY1~PY3-1.

Compound	$\lambda_{g,film}$ [a] (eV)	E_{HOMO} [b] (eV)	E_{LUMO} [c] (eV)
PY1	2.66	-5.57	-2.91
PY2	2.23	-5.60	-3.37
PY3	1.84	-5.41	-3.57
PY3-1	1.91	-5.73	-3.82

a) optical band gap was obtained from film absorption edge. b) calculated by the equation : E_{HOMO} = [- (E_{Onset} - $E_{Ferrocene}$) - 4.8]. c) LUMO level was calculated from optical band gap and HOMO level.

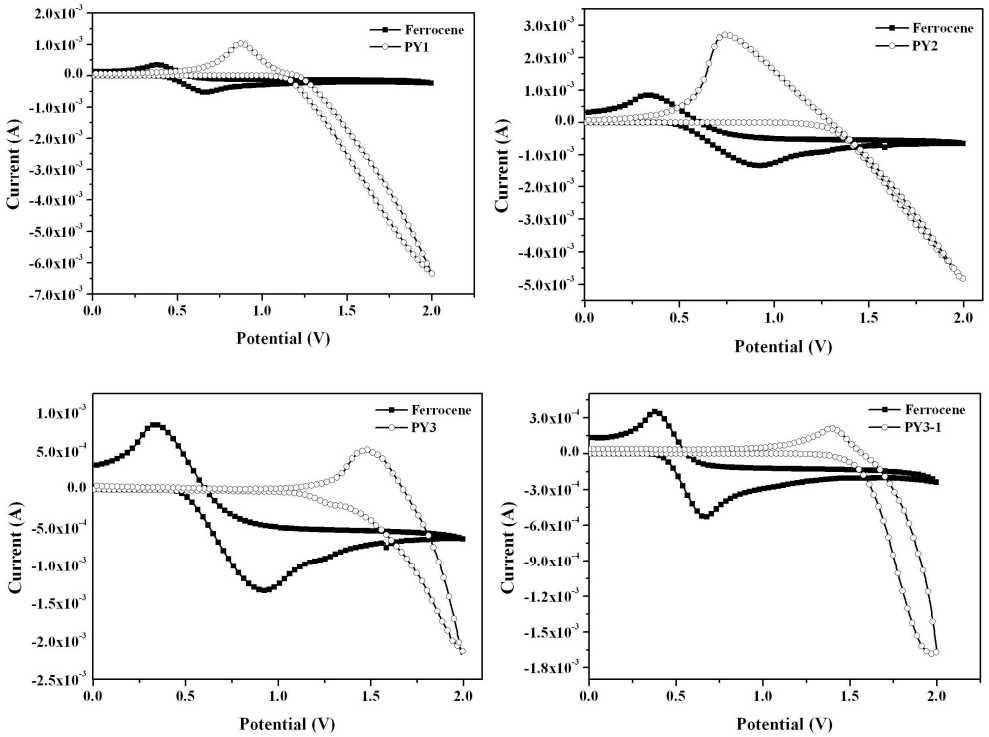

Figure 2-3. The cyclic voltammograms of PY1~PY3-1.

2-3.4. Thermal properties

The thermal properties of compound were investigated by thermogravimetric analysis (TGA) under an N_2 atmosphere (Figure 2-4, Table 2-3). All compound shows good thermal stability with with decomposition temperature (5% weight loss) of about 426, 353,383, and 344°C for PY1~PY3-1, respectively.

Table 2-3. Thermal properties of PY1~PY3-1.

Compound	T_d [a)] (°C)
PY1	426
PY2	353
PY3	383
PY3-1	344

a) measured from TGA in N_2.

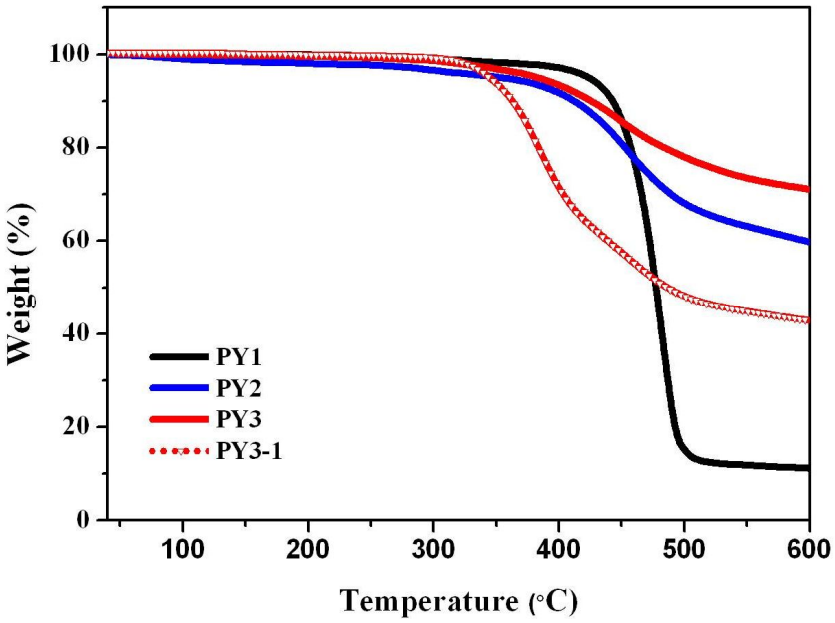

Figure 2-4. TGA traces of PY1~PY3-1.

2-3.5. Photovoltaic properties

To demonstrate the potential application of PY1~PY3-1 as a donor in OSCs, devices were fabricated with configuration ITO/PEDOT:PSS (60~70nm)/Donor:$PC_{70}BM$ blend (ca.100nm)/Al (100nm). Figure 2-5 shows the current density versus voltage (*J-V*); The data are summarized in Table 2-4. PY3 and PY3-1 showed limited device performance due to low solubility. The *J*sc for PY2 reaches value of 2.01 mA cm^{-2}, a factor of 2 times higher than for PY1. This enhanced property is attributed to acetylene-induced planarity facilitating the intermolecular interaction and enhanced light absorption at longer wavelength. Combined with increased FF (from 23.2% for PY1 to 26.6% for PY2), device of PY2/$PC_{70}BM$ (1:2 w/w) blend provided a greater PCEs (0.50%) with values *V*oc, *J*sc, and FF of 0.94 V, 2.01 mA cm^{-2}, and 26.6%, respectively than that of DPP-PY/$PC_{70}BM$ (1:4 w/w) blend (PCEs = 0.20%; *V*oc = 0.86 V; *J*sc = 1.04 mA cm^{-2}, and FF 20.0%).

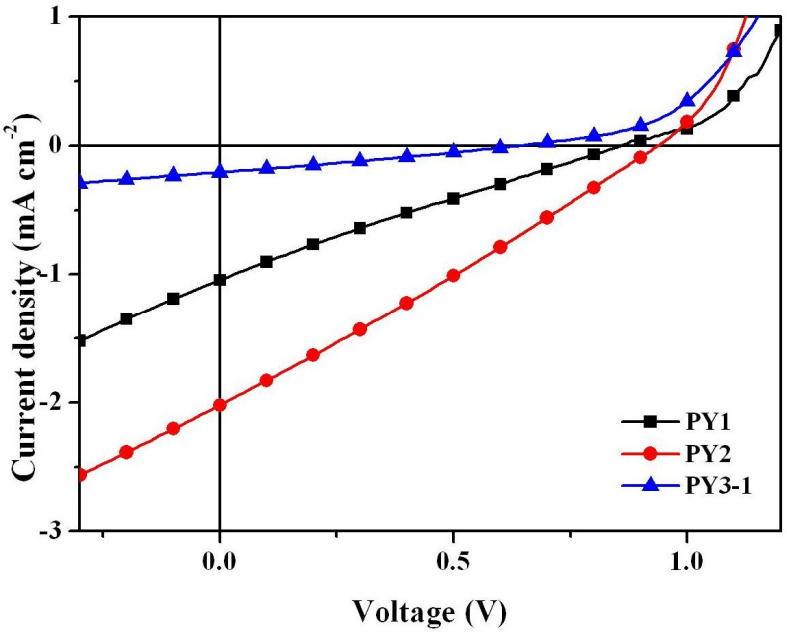

Figure 2-5. Characteristic *J*–*V* curves of solar cells fabricated from PY1~PY3-1 illuminated under AM 1.5 G, 100 mW cm^{-2}.

Table 2-4. Photovoltaic properties of PY1~PY3-1 blended with $PC_{70}BM$.
(*J*sc is the shortcircuit current density, *V*oc is the open-circuit voltage, FF is the fill factor, and PCEs is the overall power conversion efficiency.)

Compound	Blend ratio	*J*sc/ mA cm^{-2}	*V*oc/V	FF (%)	PCEs/%	Max. PCEs/%
PY1	3:7	1.04	0.86	23.2	0.12	0.20
PY2	1:2	2.01	0.94	26.6	0.46	0.50
PY3	X	X	X	X	X	X
PY3-1	7:3	0.20	0.64	20.6	0.03	0.03

2-4. Conclusion

We have developed new acetylene-incorporated pyrene derivatives in which electron-donating pyrene and electron withdrawing dicyanovinyl or octylcyanoacetate group are bridged by thienylene and acetylene group. We have observed the effects of acetylene-substitution to 1-, 3-, 6-, 8- position in pyrene revealed that these 1-, 3-, 6-, 8-acetylenic pyrene has the advantages of easy synthesis for various application, low HOMO level for high *V*oc, and planar comformation for π-π intermolecular interactions. Also, this coplanarity facilitated the internal charge transfer between electron-donating and electron-withdrawing group. However, PY3 and PY3-1 show limited device performance due low solubility. The *J*sc for PY2 reaches value of 2.01 mA cm^{-2}, a factor of 2 times higher than for PY1. This enhanced property is attributed to acetylene-induced planarity facilitating the intermolecular interaction and enhanced light absorption at longer wavelength. Combined with increased FF (from 23.2% for PY1 to 26.6% for PY2), device of PY2/$PC_{70}BM$ (1:2 w/w) blend provided a greater PCEs (0.50%) with values *V*oc, *J*sc, and FF of 0.94 V, 2.01 mA cm^{-2}, and 26.6%, respectively than that of DPP-PY/$PC_{70}BM$ (1:4 w/w) blend (PCEs = 0.20%; *V*oc = 0.86 V; *J*sc = 1.04 mA cm^{-2}, and FF 20.0%). This work demonstrates that structural modification with acetylene group can lead to positive outcome in device performances.

2-5. References

1. Kline, R. J.; McGehee, M. D.; Kadnikova, E. N.; Liu, J. S.; Frechet, J. M. J.; Toney, M. F. *Macromolecules.* **2005**, 38, 3312.

2. (a) Anthony, J. E.; Brooks, J. S.; Eaton, D. L.; Parkin, S. R. *J. Am. Chem. Soc.* **2001**, 123, 9482. (b) Dickely, K. C.; Anthony, J. E.; Loo, Y. L. *Adv. Mater.* **2006**, 18, 1721.

3. Wong, W. W. H.; Singh, T. B.; Vak, D.; Pisula, W.; Yan, C.; Feng, X.; Williams, E. L.; Chan, K. L.; Mao, Q.; Jones, D. J.; Ma, C. –Q.; Mullen, K.; Bauerle, P.; Holmes, A. B. *Adv. Funct. Mater.* **2010**, 20, 927.

4. (a) Marrocchi, A.; Silvestri, F.; Seri, M.; Facchetti, A.; Taticchi, A.; Marks, T. J. *Chem. Commun.* **2009**, 1380. (b) Silvestri, F.; Marrocchi, A.; Seri, M.; Kim, C.; Marks, T. J.; Facchetti, A.; Taticchi, A. *J. Am. Chem. Soc.* **2010**, 132, 6108.

5. (a) Qu, L.; Shi, G. *Chem. Commun.* **2004**, 2800. (b) Venkataramana, G.; Sankararaman, S. *Eur. J. Org. Chem.* **2005**, 4162. (c) Maeda, H.; Maeda, T.; Mizuno, K.; Fujimoto, K.; Shimizu, H.; Inouye, M. *Chem. Eur. J.* **2006**, 12, 824. (d) Hu, J. –Y.; Era, M.; Elsegood, M. R. J.; Yamato, T. *Eur. J. Org. Chem.* **2010**, 72. (f) Liang, Z. –Q.; Li, Y. –X.; Yang, J. –X.; Ren, Y.; Tao, X. –T. *Tetrahedron Letters*. **2011**, 52, 1329.

6. (a) Moorthy, J. N.; Natarajan, P.; Venkatakrishnan, P.; Huang, D. F.; Chow, T. J. *Org. Lett.* **2007**, 9, 2006. (b) Oh, H. –Y.; Lee, C.; Lee, S. *Organic Electronics.* **2009**, 10, 163.

(c) Sonar, P.; Soh, M. S.; Cheng, Y. H.; Henssler, J. T.; Sellinger, A. *Org. Lett.* **2010**, 12, 3292.

7. (a) Zhang, H.; Wang, Y.; Shao, K.; Liu, Y.; Chen, S.; Qiu, W.; Sun, X.; Qi, T.; Ma, Y.; Yu, G.; Su, Z.; Zhu, D. *Chem. Commun.* **2006**, 755. (b) Zophel, L.; Beckmann, D.; Enkelmann, V.; Chercka, D.; Rieger, R.; Mullen, K. *Chem. Commun.* **2011**, 47, 6960. (c) Kim, Y. S.; Bae, S. Y.; Kim, K. H.; Lee, T. W.; Hur, J. A.; Hoang, M. H.; Cho, M. J.; Kim, S. –J.; Kim, Y.; Kim, M.; Lee, K.; Lee, S. J.; Choi, D. H. *Chem. Commun.* **2011**, 47, 8907.

8. (a) Sharma, G. D.; Suresh, P.; Mikroyannidis, J. A.; Stylianakis, M. *J. Mater. Chem.* **2010**, 20, 561. (b) Lee, O. P.; Yie, A. T.; Beaujuge, P. M.; Woo, C. H.; Holcombe, T. W.; Millstone, J. E.; Douglas, J. D.; Chen, M. S.; Frechet, J. M. J. *Adv. Mater.* **2011**, 23, 5359.

9. (a) Vollmann, H.; Becker, H.; Corell, M.; Streeck, H. *Liebigs Ann.* **1937**, 531, 1. (b) Altschuler, L.; Berliner, E. *J. Am. Chem. Soc.* **1966**, 88, 5837. (c) Dewar, M. J. S.; Dennington, R. D. *J. Am. Chem. Soc.* **1989**, 111, 3804.

CHAPTER 3.
Mono-functionalized Pyrene Derivatives for Bulk-heterojunction Organic Solar Cells

3-1. Introduction

Developing small molecule organic solar cells (SMOSCs) has emerged as one of the most promising research field due to their advantages such as versatility in molecular design, perfectly defined chemical structure, easy purification, and reproducibility without batch to batch variation.[1] Based on these advantages, the tremendous effort has been devoted to develop appropriate donor materials for SMOSCs.[2] Among them, donor-acceptor-donor (D-A-D) type triad molecule incorporating intra-molecular charge transfer characteristics via covalent bonding of electron donor and acceptor has emerged as a promising molecular architecture for high performance SMOSCs.[3] Recently, Frechet et al. reported various D-A-D triad molecules using 1,4-diketo-3,6-dithienylpyrrolo[3,4-c]pyrrole (DPP) as an efficient acceptor moiety.[4] In particular, pyrene-DPP-pyrene triad, with thienylene connection to either 1- or 2-position of pyrenes, was developed to show high power conversion efficiencies (PCEs): over 4% PCEs was obtained for 2-pyrene triad while only 0.7% PCEs was obtained for 1-pyrene triad. However, it should be noted that the 2-pyrene substitution is very much

complicated and inefficient in synthesis due to the preferential activation of 1-position for the electrophilic aromatic substitution.[5]

To further increase the PCEs of pyrene-DPP-pyrene triad in this work, we decided to insert acetylene linkage between pyrene and DPP. The acetylene-incorporation was intended to benefit reduced highest occupied molecular orbital (HOMO)-lowest unoccupied molecular orbital (LUMO) band gap through extended conjugation, and also the increased ionization potential of the triad molecule based on the relatively larger electron-withdrawing characteristics of *sp*-hybridization over sp^2-hybridization.[6] It is well known that the former is effective in increasing short-circuit current (*J*sc), while the latter in increasing open-circuit voltage (*V*oc).[6] To explore such effects of acetylene insertion, we designed synthetically more feasible 1-pyrene triads with and without acetylene linkers (DPP-A-PY(OD/HD) and DPP-PY, respectively).

3-2. Experimental

3-2.1. Synthesis

Synthesis of DPP-A-PY(OD/HD) was done according to the pathway shown in Scheme2, while that of DPP-PY was due to the literature procedure.[4] Compound 1, synthesized through a known procedure[7], was reacted with alkyl halide and K_2CO_3 in 18-crown-6 and DMF to give compound 2. Compound 3 was readily synthesized through bromination of 2 with NBS. Compound 4 was obtained through Sonogashira reaction of 1-bromopyrene and trimethylsilylacetylene, which was subsequently treated with K_2CO_3 in MeOH and THF to afford 5. The final product, DPP-A-PY(OD/HD), was synthesized through Sonogashira reaction of 3 and 5, while DPP-PY was synthesized according to the reported procedure.[4] Both DPP-A-PY(OD/HD) and DPP-PY were highly soluble in common organic solvents such as $CHCl_3$, THF and CB, which enabled the solution process for organic solar cell (OSC) fabrication.

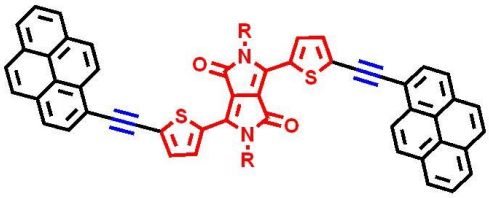

R : 2-octyldodecyl (OD)
2-hexyldecyl (HD)

DPP-A-PY(OD/HD)

R : 2-octyldodecyl

DPP-PY

Scheme 3-1. Chemical structures of DPP-A-PY(OD/HD) and DPP-PY.

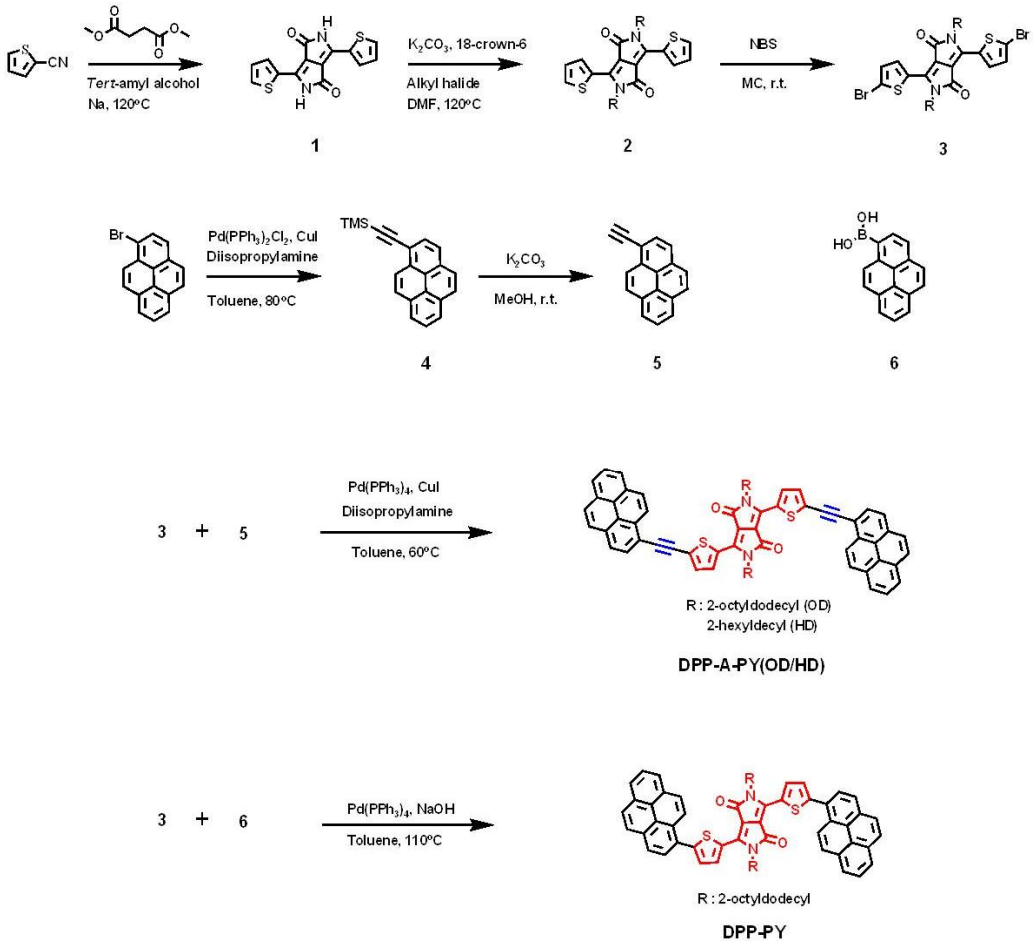

Scheme 3-2. Synthesis of DPP-A-PY(OD/HD) and DPP-PY.

3,6-di(thiophen-2-yl)pyrrolo[3,4-c]pyrrole-1,4(2H,5H)-dione (1)

Sodium metal (1.21g, 52.64mmol) immersed in mineral oil was washed with hexanes and cut into small pieces. Sodium metal pieces were slowly added to the solution of tert-amyl alcohol (40ml) under Ar atmosphere. The mixture was slowly heated to 120℃

and stirred for overnight. Then 2-thiophenecarbonitrile (2.18, 26.32mmol) was added and dimethylsuccinate (1.83g, 10.53mmol) was added dropwise to the reaction mixture for 1h. The mixture was stirred at 120℃ for 3h and then cooled to room temperature. The contents were poured into acidic MeOH (200ml MeOH and 10ml HCl) in ice bath and stirred for 1.5h. Filtration of the suspension yielded a purple solid (2.13g, 33.9%), which was used in next step without further purification.

2,5-bis(2-octyldodecyl)-3,6-di(thiophen-2-yl)pyrrolo[3,4-c]pyrrole-1,4(2H,5H)-dione (2)

3,6-di(thiophen-2-yl)pyrrolo[3,4-c]pyrrole-1,4(2H,5H)-dione (1) (2.28g, 8.51mmol), K_2CO_3 (3.88g, 28.08mmol), 18-crown-6 (0.25g, 0.94mmol), and DMF (70ml) were added to two-necked round bottom flask. The reaction mixture was stirred at 120℃ for 3h and 2-octyldodecyl iodide (10.14g, 28.07mmol) solvated in DMF (20ml) was added dropwise to the reaction. The mixture was heated at 120℃ for 3days and then cooled to room temperature. The contents were poured into water and extracted with diethyl ether. The organic layer was then dried over $MgSO_4$. After evaporation of the solvent, the residue was purified by column chromatography on a silica gel ($CHCl_3$/n-Hex = 1:4) and reprecipitation using MC/MeOH to afford purple solid (1.1g, 19.3%). ^{1}H NMR (300MHz, $CDCl_3$, δ) : 8.76 (d, 2H), 7.61 (d, 2H), 7.27 (dd, 2H), 4.01 (d, 4H), 1.90-1.88 (m, 2H), 1.27-1.20 (m, 64H), 0.89-0.83 (m, 12H).

3,6-bis(5-bromothiophen-2-yl)-2,5-bis(2-octyldodecyl)pyrrolo[3,4-c]pyrrole-1,4(2H,5H)-dione (3)

NBS (0.29g, 1.65mmol) was added dropwise to the solution of 2,5-bis(2-octyldodecyl)-3,6-di(thiophen-2-yl)pyrrolo[3,4-c]pyrrole-1,4(2H,5H)-dione (2) (0.62g, 0.71mmol) in MC (50ml) under exclusion of light. The mixture was slowly heated to room temperature and stirred for 3h. The solution was poured into water and extracted with MC. The organic layer was then dried over anhydrous $MgSO_4$. After removing the solvent, the residue was purified by column chromatography on a silica gel (EA/n-Hex=1:9) and reprecipitation using MC/MeOH to afford a dark purple solid (0.4g, 55%). ^{1}H NMR (300MHz, $CDCl_3$, δ) : 8.62 (d, 2H), 7.22 (d, 2H), 3.92 (d, 4H), 1.87 (m, 2H), 1.27-1.21 (m, 64H), 0.92-0.83 (m, 12H).

Trimethyl(pyren-1-ylethynyl)silane (4)

The mixture of 1-bromopyrene (1.10g, 3.91mmol), $PdCl_2(PPh_3)_2$ (0.55g, 0.78mmol), and CuI (14.9g, 0.78mmol) in diisopropylamine(30ml) and toluene(15ml) were stirred at 0℃ under Ar atmosphere for 30min. Then trimethylsilylacetylene (1.65ml, 11.73mmol) was added to the mixture and stirred at 80℃ for 24h. After evaporation of the solvent, the residue was purified by column chromatography on a silica gel (n-Hex) to afford a yellow solid (1.0g, 82%). ^{1}H NMR (300MHz, $CDCl_3$, δ) : 8.56 (d, 1 H),

8.24-8.00 (m, 8 H), 0.39 (s, 9 H).

1-ethynylpyrene (5)

To a solution of trimethyl(pyren-1-ylethynyl)silane (4) (0.30g, 1.00mmol) in MeOH (10ml) and THF (10ml) was treated with K_2CO_3 (0.69g, 5.02mmol). The solution was stirred for 12h at room temperature. After removing the solvent, the residue was purified by column chromatography on a silica gel ($CHCl_3$) and recrystallized using $CHCl_3$ to afford a brown solid (0.21g, 92%). ^{1}H NMR (300MHz, $CDCl_3$, δ) : 8.59 (d, 1 H), 8.24-8.01 (m, 8 H), 3.62 (s, 1 H)

2,5-bis(2-octyldodecyl)-3,6-bis(5-(pyren-1-ylethynyl)thiophen-2-yl)pyrrolo[3,4-c] pyrrole -1,4(2H,5H)-dione (DPP-A-PY(OD))

3,6-bis(5-bromothiophen-2-yl)-2,5-bis(2-octyldodecyl)pyrrolo[3,4-c]pyrrole-1,4(2H,5H)-dione (3) (250mg, 0.24mmol), CuI (3.5mg, 0.018mmol), and $Pd(PPh_3)_4$ (21.3mg, 0.018mmol) in diisopropylamine (2.3ml) and toluene (5.1ml) were stirred under Ar atmosphere at 0°C for 30min. 1-ethynylpyrene (5) was then added, and the mixture was heated to 60°C for 24 h. The mixture was poured into water and extracted with $CHCl_3$. The organic layer was then dried over anhydrous $MgSO_4$. After evaporation of the solvent, the residue was purified by column chromatography on a silica gel ($CHCl_3$/n-Hex = 2:8 → $CHCl_3$) and recrystallization using EA to afford a

dark violet solid (0.21g, 65%). ^{1}H NMR (300MHz, $CDCl_3$, δ) : 8.99 (d, 2 H), 8.61 (d, 2H) 8.27-8.03 (m, 16 H), 7.55 (d, 2 H), 4.10 (d, 4H), 2.03 (m, 2H), 1.39-1.20 (m, 64H), 0.81 (m, 12H). ^{13}C NMR (500MHz, $CDCl_3$, δ) : 161.4, 139.3, 135.7, 132.9, 131.8, 131.2, 130.9, 130.7, 129.4, 128.7, 127.1, 126.3, 125.8, 125.1, 124.4, 116.6, 108.9, 97.4, 88.0, 46.5, 37.9, 31.9, 31.3, 30.1, 29.6, 29.3, 26.3, 22.6, 14.0. High-resolution mass spectrometry (HRMS) (positive electron ionization (EI+)) mass-to-charge ratio (m/z) : $[M+H]^+$ calculated for $C_{90}H_{105}N_2O_2S_2$, 1309.76 ; found 1309.76. Elemental Analysis calculated for $C_{90}H_{104}N_2O_2S_2$: C 82.52, H 8.00, N 2.14, O 2.44, S 4.90; found: C 82.45, H 8.06, N 2.15, O 2.41, S 5.05.

2,5-bis(2-hexyldecyl)-3,6-bis(5-(pyren-1-ylethynyl)thiophen-2-yl)pyrrolo[3,4-c] pyrrole -1,4(2H,5H)-dione (DPP-A-PY(HD))

3,6-bis(5-bromothiophen-2-yl)-2,5-bis(2-hexyldecyl)pyrrolo[3,4-c]pyrrole-1,4(2H,5H)-dione (3) (250mg, 0.24mmol), CuI (3.5mg, 0.018mmol), and $Pd(PPh_3)_4$ (21.3mg, 0.018mmol) in diisopropylamine (2.3ml) and toluene (5.1ml) were stirred under Ar atmosphere at 0°C for 30min. 1-ethynylpyrene (5) was then added, and the mixture was heated to 60°C for 24 h. The mixture was poured into water and extracted with $CHCl_3$. The organic layer was then dried over anhydrous $MgSO_4$. After evaporation of the solvent, the residue was purified by column chromatography on a silica gel ($CHCl_3$/n-Hex = 2:8 → $CHCl_3$) and recrystallization using EA to afford a

dark violet solid (0.23g, 69%). ^{1}H NMR (300MHz, $CDCl_3$, δ) : 8.99 (d, 2 H), 8.61 (d, 2H) 8.27-8.03 (m, 16 H), 7.55 (d, 2 H), 4.10 (d, 4H), 2.03 (m, 2H), 1.39-1.20 (m, 48H), 0.81 (m, 12H). ^{13}C NMR (500MHz, $CDCl_3$, δ) : 161.4, 139.3, 135.69, 132.9, 131.8, 130.9, 129.4, 128.7, 127.1, 126.3, 125.8, 124.3, 116.6, 108.9, 97.4, 88.0, 46.4, 37.8, 31.8, 31.3, 30.0, 29.5, 26.2, 22.6, 14.0. High-resolution mass spectrometry (HRMS) (positive electron ionization (EI+)) mass-to-charge ratio (m/z) : $[M+H]^+$ calculated for $C_{82}H_{89}N_2O_2S_2$, 1197.63 ; found 1197.63. Elemental Analysis calculated for $C_{82}H_{88}N_2O_2S_2$: C 82.23, H 7.41, N 2.34, O 2.67, S 5.35; found: C 82.27, H 7.46, N 2.35, O 2.60, S 5.39.

2,5-bis(2-octyldodecyl)-3,6-bis(5-(pyren-1-yl)thiophen-2-yl)pyrrolo[3,4-c]pyrrole-1,4(2H,5H)-dione (DPP- PY)

3,6-bis(5-bromothiophen-2-yl)-2,5-bis(2-octyldodecyl)pyrrolo[3,4-c]pyrrole-1,4(2H,5H)-dione (3) (300mg, 0.29mmol), pyren-1-ylboronic acid (297mg, 1.20mmol), $Pd(PPh_3)_4$ (34mg, 0.03mmol), toluene (10ml), EtOH (3ml), and NaOH (2N) (2.5ml) were added to a two-necked round bottom flask under Ar atmosphere. The solution was stirred at 110°C for 24h. The mixture was poured into water and extracted with $CHCl_3$. The organic layer was then dried over anhydrous $MgSO_4$. After evaporation of the solvent, the residue was purified by column chromatography on a silica gel ($CHCl_3$/n-Hex = 2:8 → $CHCl_3$) and being precipitated into MeOH to afford a dark violet solid

(100mg, 27%). ^{1}H NMR (300MHz, $CDCl_3$, δ) : 9.16 (d, 2 H), 8.57 (d, 2H) 8.26-8.03 (m, 16 H), 7.60 (d, 2 H), 4.16 (d, 4H), 2.13 (m, 2H), 1.40-1.18 (m, 64H), 0.82 (m, 12H). ^{13}C NMR (500MHz, $CDCl_3$, δ) : 161.9, 148.4, 140.1, 136.2, 131.7, 131.4, 130.9, 130.4, 129.3, 129.0, 128.5, 128.2, 127.2, 126.3, 125.7, 125.4, 125.1, 124.7, 124.5, 108.2, 46.5, 38.0, 31.8, 31.4, 30.1, 29.6, 29.3, 26.4, 22.6, 14.0. High-resolution mass spectrometry (HRMS) (positive electron ionization (EI+)) mass-to-charge ratio (m/z) : $[M+H]^+$ calculated for $C_{86}H_{105}N_2O_2S_2$, 1261.76 ; found 1261.76. Elemental Analysis calculated for $C_{86}H_{104}N_2O_2S_2$: C 81.86, H 8.31, N 2.22, O 2.54, S 5.08; found: C 81.56, H 8.33, N 2.18, O 2.88, S 4.99.

3-2.2. Instruments and measurements

Chemical structures were fully identified by ^{1}H NMR (Bruker, Avance-300), ^{13}C NMR (Bruker, Avance 500), GC-Mass (JEOL, JMS-700), and elemental analysis (EA1110, CE Instrument). The melting temperatures of the compounds were determined using DSC under an N_2 atmosphere, using a TA instruments Q1000 model. The decomposition temperatures of the compounds were obtained using TGA under an N_2 atmosphere, using a TA instruments Q50 model. UV-Vis spectra were recorded on a SHIMADZU UV-1650PC. HOMO level was obtained from the cyclic voltammetry measurements. Cyclic voltammetric measurements were performed using a 273A (Princeton Applied Research) with a one-compartment electrolysis cell consisting of a

platinum working electrode, a platinum wire counter-electrode, and a quasi Ag+/Ag electrode as reference. Measurements were performed in a 0.5 mM acetonitrile solution with tetrabutylammonium tetrafluoroborate as the supporting electrolyte, at a scan rate of 50 mV/s. Each oxidation potential was calibrated using ferrocene as a reference. LUMO level was calculated from the HOMO level and the optical band gap, which was obtained from the edge of the absorption spectra.

3-2.3. Fabrication and characterization of organic solar cells (OSCs)

The organic solar cells in this study were fabricated by following method. Patterned ITO glass substrates (~10Ω/square) were cleaned in an ultrasonic bath with trichloroethylene, acetone, isopropyl alcohol for 10 minute, respectively and then blow dried with a N_2 stream. A 30nm of PEDOT:PSS (AI P 4083) was then spin-coated on to the substrate (5000rpm / 30s). The films were dried at 150°C for 20min. Subsequently, the DPP-A-PY : $PC_{70}BM$ (> 99.0%, ADS) solutions were deposited through spin casting at 1000 rpm / 40s. The thickness of DPP-A-PY : $PC_{70}BM$ films were around 130 nm. Al electrodes were deposited via thermal evaporation with thickness of 100nm. The active area of these solar cells was 0.09 cm^2.

The current density-voltage (*J-V*) characteristics of the solar cells were measured with a Keithley 4200 source measurement unit. The solar cell performances were characterized under AM1.5G condition with an illumination intensity of 100 mW cm^{-2}

generated by a Oriel Sol 3A solar simulator. *J-V* characteristics of the cells with illumination were measured using a metal mask of 0.09 cm^2. The intensity dependent measurements have been performed with various neutral density filters.

Incident photon to current conversion efficiency (IPCE) was measured using Oriel QE/IPCE Measurement Kit which composed of 300W Xenon Lamp, monochromator (74125), the order sorting filter wheel, the Merlin lock-in amplifier (70104) and the chopper.

3-3. Result and Discussion

3-3.1. Density functional theory (DFT) calculation

Theoretical molecular orbital calculation was carried out using Gaussian09 at B3LYP/6-31G* level to characterize optimized ground state geometry and electron density of HOMO and LUMO states. In optimized ground state geometry, DPP-A-PY showed planar non-twisted conformation due to small torsion angle between pyrene and thiophene moiety than that of DPP-PY (5.7 ° ~5.9 ° for DPP-A-PY and 38.0 ° ~50.1 ° for DPP-PY) (Figure 3-1).[8] The coplanarity facilitates the internal charge transfer between electron-donating pyrene and electron-withdrawing DPP group. Overall conjugation length of DPP-A-PY is relatively increased in comparison with that of DPP-PY (Figure 3-2) and thereby the band gap is reduced (Table 3-1). As the DPP moiety holds strong tendancy of π-π stacking[7], this structural planarity would synergetically reinforce the intermolecular interaction between neighboring molecules to give enhance transport property of DPP-A-PY compared to that of DPP-PY.

(a) DPP-A-PY

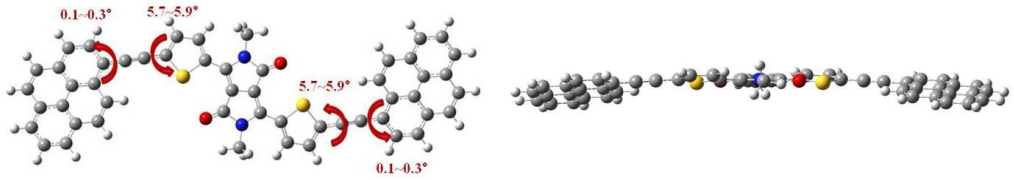

(b) DPP-PY

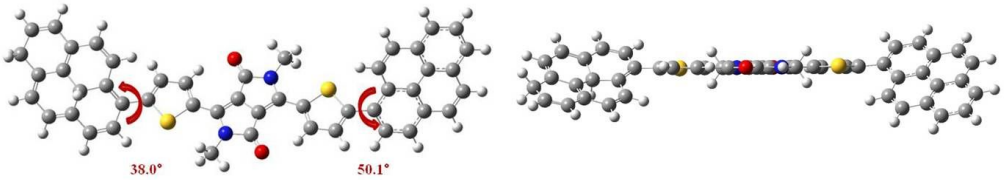

Figure 3-1. The calculated optimized ground state geometry of (a) DPP-A-PY and (b) DPP-PY. Top view and front view obtained using Gaussian 09 at the B3LYP/6-31G* level.

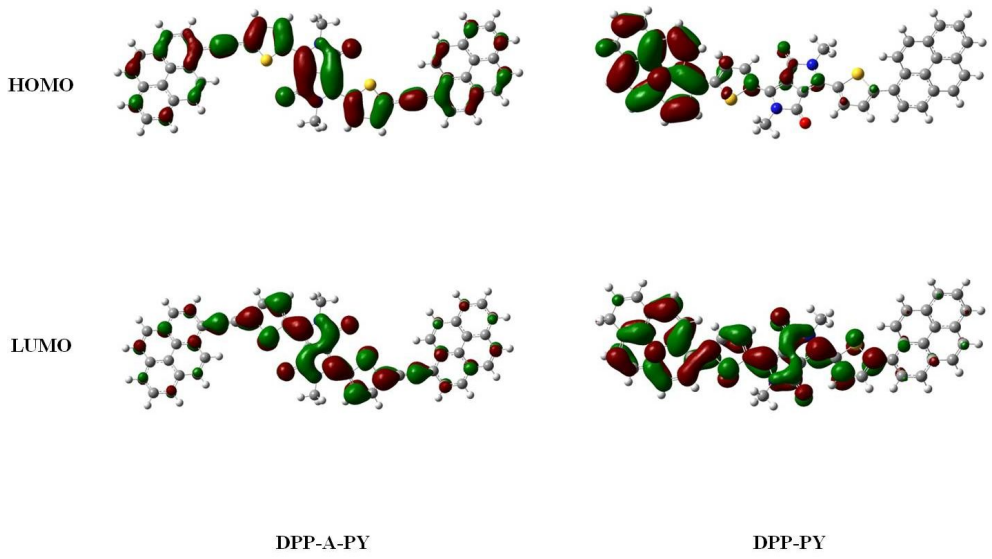

Figure 3-2. The calculated HOMO and LUMO energy density maps of DPP-A-PY and DPP-PY obtained using Gaussian 09 at the B3LYP/6-31G* level.

3-3.2. Optical properties

Figure 3-3 shows (a) the UV-Vis absorption spectra of DPP-A-PY(OD) and DPP-PY in $CHCl_3$ solution, and (b) those of spin-coated film from $CHCl_3$ solution; Table 3-1 lists the measured data. It is noted that DPP-A-PY(OD) exhibits the red shifted and broadened absorption spectrum than that of DPP-PY in solution. Furthermore, DPP-A-PY(OD) shows higher molar extinction coefficients of 59,400 M^{-1} cm^{-1} at 632nm (cf. 42,300 M^{-1} cm^{-1} at 590nm for DPP-PY). The film spectra of both compounds show red-shifted absorption relative to the solution spectra, which is originated from structural reorganization and intermolecular stacking in the solid state.[10] The film of DPP-A-PY(OD) shows vibrationally resolved absorption spectrum which extends into the near IR region (~750nm) with absorption band maximum at 685nm. Very distinctive and featured absorption at 685nm in DPP-A-PY(OD) indicates that incorporation of acetylene π-spacer results in more planar structure and strong intermolecular interactions.[9] In fact, the optical band gap estimated from the absorption edge of DPP-A-PY(OD) (1.69 eV) in thin film is smaller than that of DPP-PY (1.78 eV). Bathochromically shifted absorption onset and reduced optical band gap of DPP-A-PY(OD) in film state are consistent with the DFT calculation (*vide supra*) and attests the role of acetylene linker in extending the conjugation and planarization.

(a) In solution

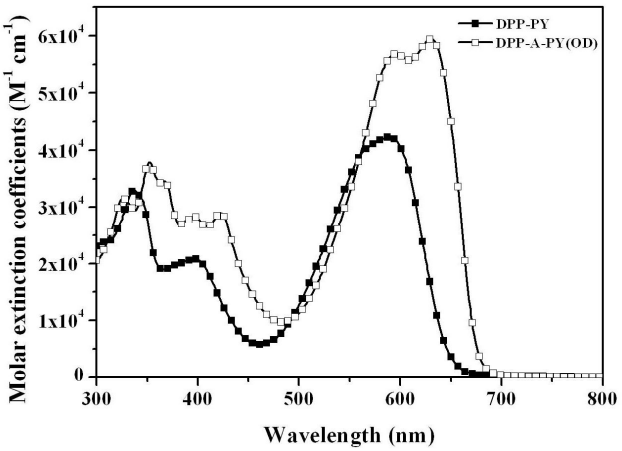

(b) In film

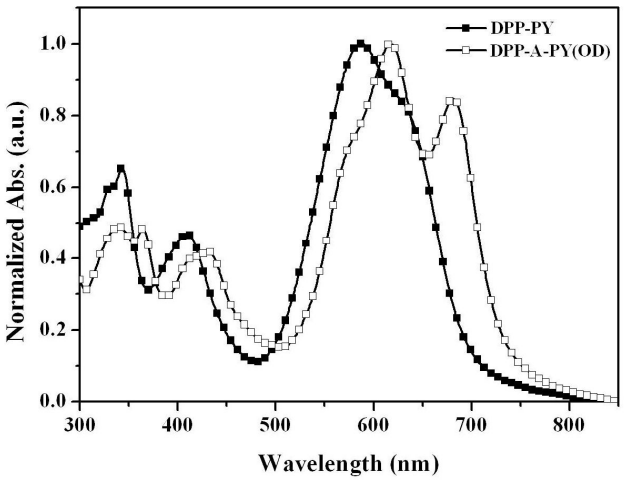

Figure 3-3. The normalized UV-Vis absorption spectra of compound DPP-A-PY(OD) and DPP-PY in (a) $CHCl_3$ solution and (b) spincoated film from $CHCl_3$ solution.

Table 3-1. Optical properties of DPP-A-PY(OD) and DPP-PY.

Compound	$\lambda_{abs,sol}$ [a] (nm)	$\lambda_{abs,film}$ [b] (nm)	$\lambda_{onset,film}$ (nm)	$\lambda_{g,film}$ [c] (eV)
DPP-A-PY(OD)	352, 423, 595, 632	364, 428, 618, 682	733	1.69
DPP-PY	338, 397, 590	343, 410, 590	695	1.78

a) Measured in chloroform solution of concentration of 10^{-5}M. b) Spin-coated from 0.5wt% chloroform solution. c) Optical band gap was obtained from film absorption edge.

3-3.3. Electrochemical properties

The electrochemical properties of both compounds in thin film were investigated using cyclic voltammetry (LUMO energy level was calculated from optical band gap and the electrochemically measured HOMO energy level, see Figure 3-4). The HOMO and LUMO energy levels of DPP-A-PY(OD) and DPP-PY were -5.72/-4.03 eV and -5.51/-3.73 eV, respectively. Consistent with our expectation and also with the DFT calculation results, the introduction of acetylene moiety between pyrene and DPP clearly lowered the HOMO energy level, which is beneficial for high *V*oc (The data are summarized in Table 3-2).[6]

Table 3-2. Electrochemical properties of DPP-A-PY(OD) and DPP-PY.

Compound	$\lambda_{g,film}$ [a] (eV)	E_{HOMO} [b] (eV)	E_{LUMO} [c] (eV)
DPP-A-PY(OD)	1.69	-5.72	-4.03
DPP-PY	1.78	-5.51	-3.73

a) optical band gap was obtained from film absorption edge. b) calculated by the equation : E_{HOMO} = [- (E_{Onset} - $E_{Ferrocene}$) - 4.8]. c) LUMO level was calculated from optical band gap and HOMO level.

(a) DPP-A-PY(OD)

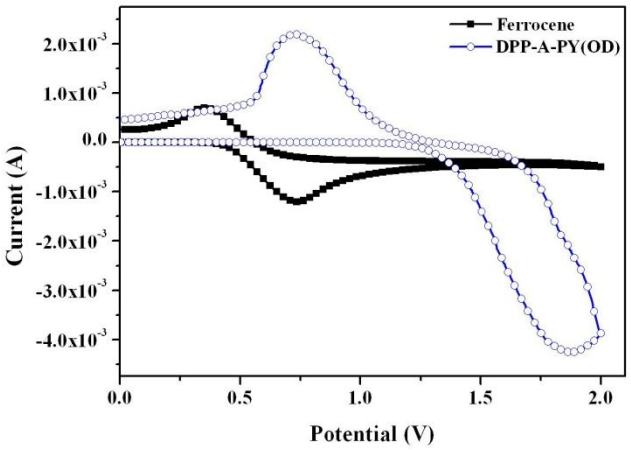

(b) DPP-PY

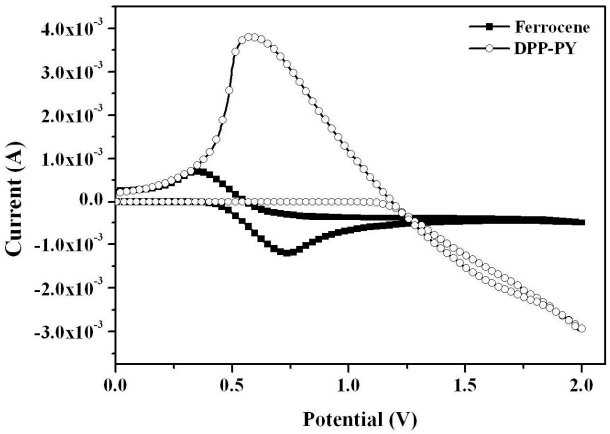

Figure 3-4. The cyclic voltammograms of (a) DPP-A-PY(OD) and (b) DPP-PY.

3-3.4. Thermal properties

The thermal property of both compounds was investigated by thermogravimetric analysis (TGA) under an N_2 atmosphere (see Figure 3-5, Table 3-3). DPP-A-PY(OD) exhibits better thermal stability with decomposition temperature (5% weight loss) of about 407˚C than DPP-PY (360°C), again indicating the positive role of acetylene group.

Table 3-3. Thermal properties of DPP-A-PY(OD) and DPP-PY.

Compound	T_d [a)] (°C)
DPP-A-PY(OD)	407
DPP-PY	360

a) measured from TGA in N_2.

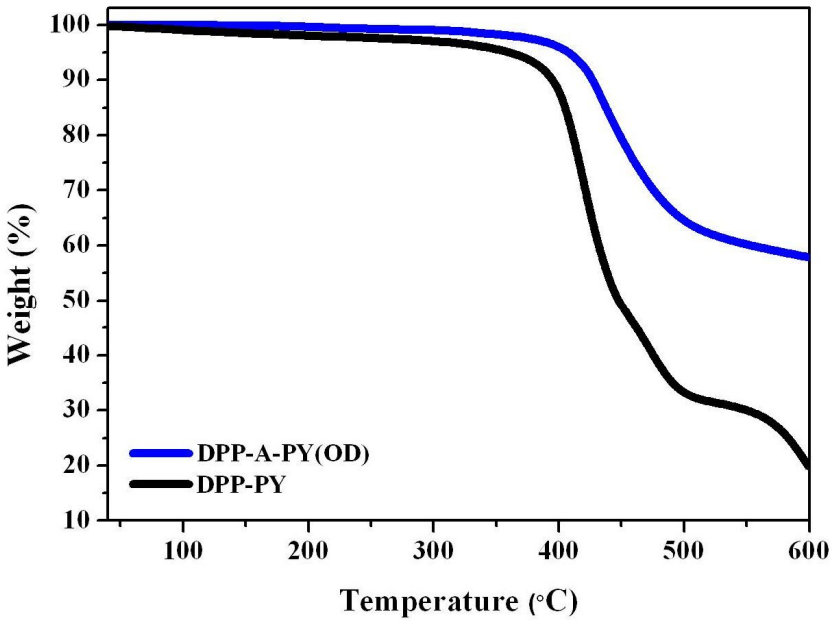

Figure 3-5. TGA traces of DPP-A-PY(OD) and DPP-PY.

3-3.5. Photovoltaic properties

To demonstrate the potential application of DPP-A-PY(OD/HD) as a donor in solution-processed OSCs, devices were fabricated with configuration of ITO/PEDOT:PSS (30~40nm)/DPP-A-PY(OD/HD):$PC_{70}BM$ blend (ca.100nm)/Al (100nm). The same devices with DPP-PY:$PC_{70}BM$ as an active layer were also fabricated as a control according to previously reported procedure.[4] Optimal DPP-A-PY(OD/HD):$PC_{70}BM$ devices were obtained when using $CHCl_3$ solutions at a concentration of 20mg/mL with DPP-A-PY(OD/HD):$PC_{70}BM$ blending ratio of 7:3 by weight. Optimized DPP-A-PY(OD/HD):$PC_{70}BM$ devices were annealed after cathode deposition at 100°C for 5min. Figure 3-6 and 3-7 shows the current density versus voltage (*J-V*) and incident-photon conversion efficiency (IPCE) characteristics. It is first noted that the *V*oc for DPP-A-PY(OD/HD) is distinctively higher than that of DPP-PY by ~0.1 eV. This increased *V*oc is consistent with the lowered HOMO energy level of DPP-A-PY(OD) (5.72eV) compared to that of DPP-PY (5.51eV). Most evidently, *J*sc for DPP-A-PY(OD/HD) has significantly increased from that for DPP-PY; 6.20/8.89 mA cm^{-2}, a factor of about 2- /3- times higher than that. This enhanced property is attributed to acetylene-induced planar back-bone facilitating the intermolecular interaction and enhanced absorption at longer wavelength. Combined with increased FF (from 27.2% for DPP-PY to 41.9/41.7% for DPP-A-PY(OD/HD)), device of DPP-A-PY(OD/HD)/$PC_{70}BM$ (7:3 w/w) blend provided a greater PCEs (2.25/3.15%) with

values *V*oc, *J*sc, and FF of 0.87/0.85 V, 6.20/8.89 mA cm^{-2}, and 27.2/41.7%, respectively than that of DPP-PY/$PC_{70}BM$ (1:4 w/w) blend (PCEs = 0.51%; *V*oc = 0.79 V; *J*sc = 2.38 mA cm^{-2}, and FF 27.2%). As the optimized molecular structure for the highest performance, the blend of DPP-A-PY(HD):$PC_{70}BM$ (7:3 w/w) exhibits a broad IPCE plateau between 300 and 750nm with a maximum of 46% at 577nm (The data are summarized in Table 3-4).

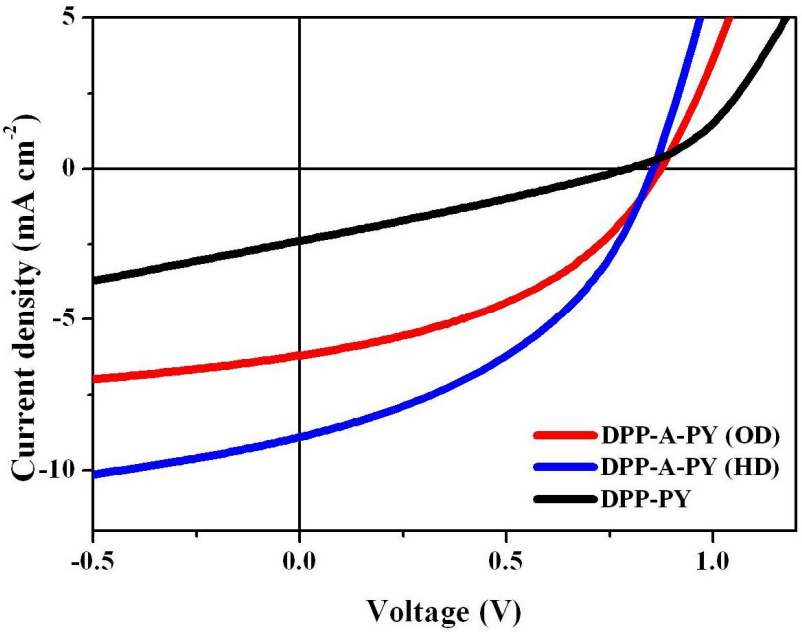

Figure 3-6. Characteristic *J–V* curves of solar cells fabricated from DPP-A-PY(OD/HD) and DPP-PY illuminated under AM 1.5 G, 100 mW cm $^{-2}$.

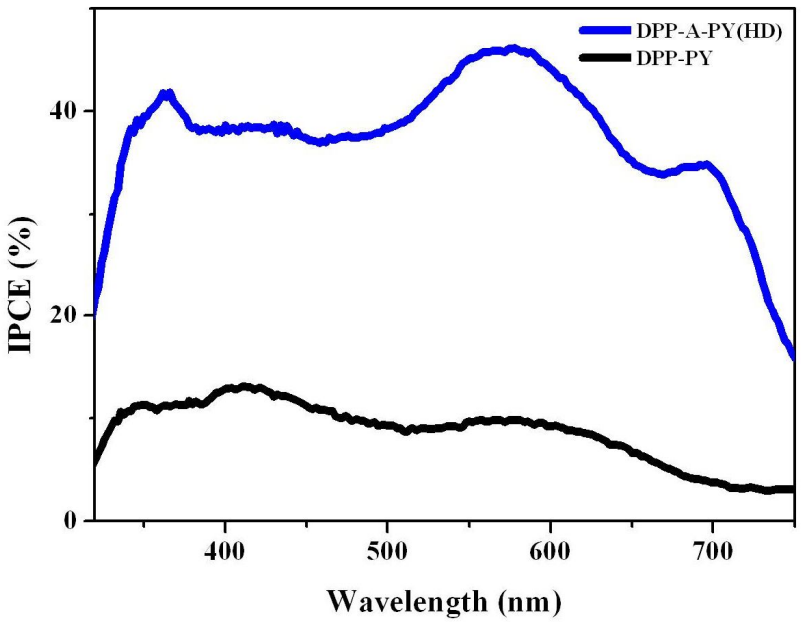

.Figure 3-7. IPCE spectrum of solar cells fabricated from DPP-A-PY(HD) and DPP-PY illuminated under AM 1.5 G, 100 mW cm^{-2} .

Table 3-4. Photovoltaic properties of DPP-A-PY(OD/HD) and DPP-PY blended with $PC_{70}BM$.

Compound (Blend ratio)	J_{sc} (mA cm^{-2})	V_{oc} (V)	FF (%)	PCEs (%)	Max. PCEs (%)
DPP-A-PY(OD) (7:3)	6.20	0.87	41.9	1.96	2.25
DPP-A-PY(HD) (7:3)	8.89	0.85	41.7	2.95	3.15
DPP-PY (1:4)	2.38	0.79	27.2	0.46	0.51

3-4. Conclusion

In conclusion, to explore the effects of acetylene-incorporation, acetylene-bridged D-A-D type small molecules (DPP-A-PY(OD/HD)) using pyrene as a donor and diketopyrrolopyrrole as an acceptor were synthesized and their photophysical, electrochemical, thermal, and photovoltaic device properties were investigated. Consistent with the expectation and DFT calculation result, DPP-A-PY (OD/HD) exhibited planar back-bone, conjugation extension, enhanced light absorption, and low HOMO energy level. Combined with the advanced properties, solution-processed OSCs based on DPP-A-PY(HD) exhibited PCEs of 3.15%. Through this work, we clearly demonstrate benefitial effect of acetylene linkage, and also, we expect that 1-ethynylpyrene can be used as an efficient donor for high performance solution-processed SMOSCs.

3-5. References

(1) (a) Roncali, J. *Acc. Chem. Res.* **2009**, 42, 1719. (b) Walker, B.; Kim, C.; Nguyen, T. -Q. *Chem. Mater,* **2011**, 23, 470. (c) Mishra, A.; Bauerle, P. *Angew. Chem. Int. Ed.* **2012**, 51, 2020.

(2) (a) Li, Y.; Guo, Q.; Li, Z.; Pei, J.; Tian, W.; *Energy Environ. Sci*. **2010**, 3, 1427. (b) Shang, H.; Fan, H.; Liu, Y.; Hu, W.; Li, Y.; Zhan, X. *Adv. Mater.* **2011**, 23, 1554. (c) Lin, L. -Y.; Chen, Y. -H.; Huang, Z. -Y.; Lin, H. -W.; Chou, S. -H.; Lin. F.; Chen, C. -W.; Liu, Y. -H.; Wong, K. -T. *J. Am. Chem. Soc*. **2011**, 133, 15822. (d) Sun, Y. M.; Welch, G. C.; Leong, W. L.; Takacs, C. J.; Bazan, G. C.; Heeger, A. J. *Nat. Materials.* **2012**, 11, 44.

(3) (a) Walker, B.; Tamayo, A. B.; Dang, X. -D.; Zalar, P.; Seo, J. H.; Garcia, A.; Tantiwiwat, M.; Nguyen, T. -Q. *Adv. Funct. Mater*. **2009**, 19, 3063. (b) Velusamy, M.; Huang, J. -H.; Hsu, Y. -C.; Chou, H. -H.; Ho, K. -C.; Wu, P. -L.; Chang, W. -H.; Lin, J. T.; Chu, C. -W. *Org. Lett.* **2009**, 11, 4898. (c) Mei, J.; Graham, K. R.; Stalder, R.; Reynolds, J. R. *Org. Lett.* **2010**, 12, 660.

(4) Lee, O. P.; Yie, A. T.; Beaujuge, M. P.; Woo, C. H.; Holcombe, T. W.; Millstone, J. E.; Douglas, J. D.; Chen, M. S.; Frechet, J. M. J. *Adv. Mater.* **2011**, 23, 5359.

(5) (a) Altschuler, L.; Berliner, E. *J. Am. Chem. Soc.* **1966**, 88, 5837. (b) Dewar, M. J. S.; Dennington, R. D. *J. Am. Chem. Soc.* **1989**, 111, 3804. (c) Figueira-

Duarte, T. M.; Mullen, K. *Chem. Rev.* **2011**, 111, 7260.

(6) (a) Marrocchi, A.; Silvestri, F.; Seri, M.; Facchetti, A.; Taticchi, A.; Marks, T. J. *Chem. Commun*. **2009**, 1380. (b) Silvestri, F.; Marrocchi, A.; Seri, M.; Kim, C.; Marks, T. J.; Facchetti, A.; Taticchi, A. *J. Am. Chem. Soc.* **2010**, 132, 6108. (c) Wu, Z.; Fan, B.; Xue, F.; Adachi, C.; Ouyang, J. *Sol. Energy Mater. Sol. Cells.* **2010**, 94, 2230. (d) Seri, M.; Marrocchi, A.; Bagnis, D.; Ponce, R.; Taticchi, A.; Marks, T. J.; Facchetti, A. *Adv. Mater.* **2011**, 23, 3827.

(7) Tamayo, A. B.; Walker, B.; Nguyen, T. -Q. *J. Phys. Chem. C.* **2008**, 112, 11545.

(8) Baheti, A.; Lee, C. -P.; Thomas, K. R. J.; Ho, K. -C. *Phys. Chem. Chem. Phys.* **2011**, 13, 17210.

(9) (a) Uhrich, C.; Schueppel, R.; Petrich, A.; Pfeiffer, M.; Leo, K.; Brier, E.; Kilickiran, P.; Baeuerle, P. *Adv. Funct. Mater.* **2007**, 17, 2991. (b) Turbiez, M.; Frere, P.; Allain, M.; Videlot, C.; Ackermann, J.; Roncali, J. *Chem.-Eur. J.* **2005**, 11, 3742.

초 록

파이렌-아세틸렌 구조를 이용한 유기 태양전지의 물질에 관한 연구

문 정 욱
재료공학부
The Graduate School
Seoul National University

아세틸렌이 들어감에 따른 효과를 확인하기 위해 파이렌-아세틸렌 구조의 유도체들을 Sonogashira 반응을 통해 성공적으로 합성을 하였고, 이 물질들에 대한 광물리적, 전기적, 태양전지 특성을 확인하였다. 아세틸렌을 통해 HOMO와 LUMO사이의 밴드갭을 좁혀주려 하였고 또한 HOMO레벨을 낮추려고 하였다. 이러한 특성들로 인하여 *J*sc와 *V*oc가 증가할 것으로 예상하였다. 물질 디자인 컨셉과 DFT 계산을 통해 예측한 것처럼 아세틸렌을 넣어 줌으로서 좀더 평평한 구조, conjugation 증가, 장파장대에서의 빛 흡수 증가, 낮은 HOMO레벨을 유도할 수 있었다. 결과적으로 새로운 분자 구조를 통해 3.15% 의 효율을 보이는 용액 공정

유기태양전지를 구현하였다.

주요어 : 유기 태양전지, 전자주개 물질, 아세틸렌, 파이렌

학 번 : 2010-24053

List of Presentation

1. 문정욱, 조일훈, 박수영, "1,3,6,8 - Tetrafunctionalized Pyrenes for Applications in Small Molecule Solution-Processed Bulk-Heterojunction Solar Cells", 대한화학회 제 108회 총회 및 학술발표회, Daejeon, Korea, 2011-09-28.

List of Publication

1. Jeong-Wook Mun, Illhun Cho, Donggu Lee, Won Sik Yoon, Oh Kyu Kwon, Changhee Lee and Soo Young Park, “Acetylene-incorporated D-A-D Type Small Molecule Comprising Pyrene and Diketopyrrolopyrrole for High Efficiency Organic Solar Cells”, *Org.Lett*, (in submission).